Comments on Inorganic Chemistry
Publication details, including instructions for authors and subscription information:
http://www.informaworld.com/smpp/title~content=t713455155

NMR Spectroscopy Applied to Zeolite Catalysis: Progress and Prospects

Wallace O'Neil Parker Jr.[a]
[a] Department of Physical Chemistry, EniTecnologie S.p.A., San Donato, MI, Italy

To cite this Article Parker Jr., Wallace O'Neil(2000) 'NMR Spectroscopy Applied to Zeolite Catalysis: Progress and Prospects', Comments on Inorganic Chemistry, 22: 1, 31 — 73
To link to this Article: DOI: 10.1080/02603590008050863
URL: http://dx.doi.org/10.1080/02603590008050863

NMR Spectroscopy Applied to Zeolite Catalysis: Progress and Prospects

WALLACE O'NEIL PARKER, Jr.*

Department of Physical Chemistry,
EniTecnologie S.p.A.,
20097 San Donato (MI), Italy

(Received October 20, 1999)

Recent advances in NMR spectroscopy methods for studying zeolites and their catalyzed reactions are briefly reviewed. In-situ NMR spectroscopy, with its controlled atmosphere conditions, is used to characterize the active surface sites of zeolites (highly acidic microporous molecular sieves) and to elucidate the hydrocarbon reactions they catalyze. The strong Bronsted acid sites of these catalysts, SiO(H)Al, are accessible to adsorbed molecules via well defined pore systems (0.3 to 1.2 nm). Substantial progress has been made in: obtaining high resolution NMR spectra under conditions (pressure, temperature, reagent flow) similar to real reactor conditions, developing new NMR methods for characterizing quadrupolar nuclei in solids, understanding acidity in solids and evidencing the details (intermediates, pathways, kinetics) of zeolite catalyzed chemical reactions. Some of the practical aspects and limitations in performing these studies are mentioned along with future prospects. Given its high versatility and adeptness for determining: the local structure around selected nuclei (^{2}H, ^{17}O, ^{27}Al, ^{29}Si), and the structure and dynamics of organic molecules (^{1}H, ^{13}C), NMR spectroscopy is destined to attain evermore important and far-reaching application in this field of study.

Keywords: *Acidity; Bronsted acid sites; heterogeneous catalysis; hydrocarbon transformations; in-situ; molecular sieves; NMR spectroscopy; solid state; zeolites*

* Email: nparker@enitecnologie.eni.it

Comments Inorg. Chem.
2000, Vol. 22, No. 1-2, pp. 31-73
Reprints available directly from the publisher
Photocopying permitted by license only

Abbreviations: 2D, two-dimensional, COSY, correlation spectroscopy, CP, cross-polarization, CRAMPS, combined rotation and multiple-pulse spectroscopy, CSA, chemical shift anisotropy, DICO, difference correlated exchange spectroscopy, DQF, double quantum filter, GC, gas chromatography, INADEQUATE, incredible natural abundance quantum transfer experiment, INEPT, insensitive nuclei enhanced by polarization, IR, infrared, J, scalar coupling constant (Hz), MAS, magic angle spinning, MAT, magic angle turning, MQ, multiple quantum, NMR, nuclear magnetic resonance, NOESY, nuclear Overhauser effect spectroscopy, Oh, octahedral, ppm , parts per million (dimensionless unit measure of chemical shift), QCC, quadrupolar coupling constant, REDOR, rotational-echo double resonance, SEDOR, spin-echo doublke resonance, Td, tetrahedral, TEDOR, transferred-echo double resonance, TPD, temperature programmed desorption, TRAPDOR, transfer of populations in double resonance, UV, ultraviolet, XRD, x-ray diffraction

I. INTRODUCTION

A. Zeolites

There is a concerted drive by petroleum companies to substitute homogeneous processes with heterogeneous ones. Heterogeneous catalysts are much more environmentally sound than many present day industrial hydrocarbon processes which employ massive quantities of corrosive concentrated acids.

In the early 1960's synthetic zeolites became important catalysts for the petroleum industry, as a result of their ability to "crack" heavy petroleum distillates. Today, in addition to oil refining and petrochemical catalysts, zeolites are also used in detergents, separations and adsorption applications. The latter applications result from the ion-exchange and molecular seive properties of zeolites. The internal surface areas of zeolites are quite high (e.g. 10^2-10^3 m^2/g).

Zeolites are microporous crystalline aluminosilicates with acidities orders of magnitude greater than their amorphous counterparts. Nearly 100 different structural types have been synthesized and recognized [1, 2]. Zeolites are true molecular sieves because the sizes of their internal pore systems are comparable with the dimensions of small organic molecules (ca. 1 nm). Pore structures of discrete sizes are formed by open arrangements of SiO_4 and AlO_4 tetrahedra linked by corner-shared oxygen atoms. A schematic representation of the MFI framework structure is shown in Figure 1. Zeolites with large micropores (0.60–0.70 nm diameter) such as Y and with medium micropores (0.45–0.60 nm) such as ZSM-5 (Fig. 1) have had a great economic impact on petroleum processes [3, 4].

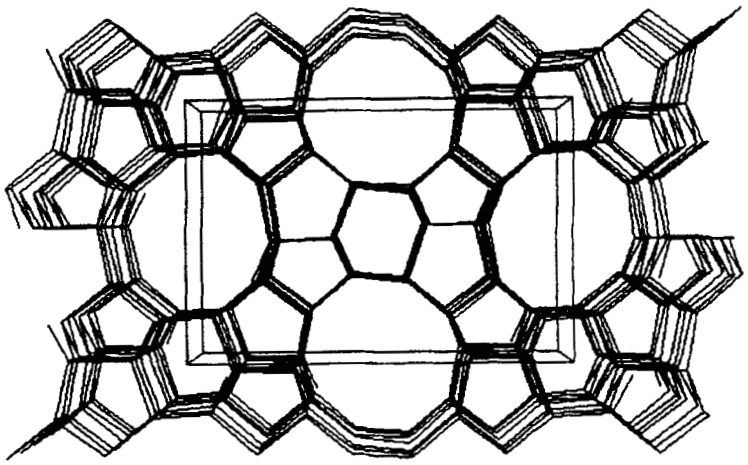

FIGURE 1 [010] Perspective view of the MFI structure looking down the linear channel system. The channels of this medium-sized micropore system are formed by 10-membered rings with free dimensions of 0.54 × 0.56 nm. For simplicity, the oxygen atoms are omitted. The unit cell is outlined and the view involves a volume element of 2 unit cells cubed. Zeolite ZSM-5 (aluminosilicalite) and silicalite-1 (pure SiO_2) have the MFI structure (Mobil type FIve)

The introduction of four-coordinate trivalent aluminum nuclei (Al^{3+}) in the framework provides a formal negative charge $[AlO_4]^-$. The cations compensating this charge during synthesis are alkali, alkaline-earth or NR_4^+ (R = H, alkyl, aryl) cations. The catalytically active acidic proton form (**H form**) of the zeolite is made by calcining off the ammonium cations or by ion-exchanging the other cations. Quaternary alkyl ammonium cations are referred to as "templates" since they can control or "direct" the microporous structure in some way. Elements other than Al can also substitute Si in the framework (e.g. B, P, Ti, Ga), but then the catalyst is not, by definition, a zeolite. Due to limited scope, these other types of crystalline catalysts will not be mentioned here.

B. NMR spectroscopy and zeolite catalysis

Homogeneous catalytic reactions are more well understood, at the molecular level, than their heterogeneous counterparts. There is a great

need to "see" the catalytically active sites on the solid surface and how the reactions actually proceed. In-situ solid state spectroscopic techniques are a powerful means for investigating these systems. NMR spectroscopy is unique, among the techniques, in that it provides information on *both* molecular structure and dynamics (albeit with rather low sensitivity). Also, NMR can be used to quantify nuclei, since signal intensities are directly proportional to concentration.

NMR studies can help determine structure-function relationships (active site structure-acidity or catalytic activity), which can ultimately allow the identification of ideal processes (catalysts, conditions) for a given molecular reaction. To fully understand catalysis at the molecular level, the following objectives must be realized.

a) Characterize active sites: determine their nature, amounts, and strengths.

b) Determine pathways (reagents, intermediates, products) and relative reaction rates.

c) Determine roles of active sites in various reactions, connecting acidity and catalysis.

In-situ NMR spectroscopy can investigate: the active surface sites directly (section IV, A) or with molecular probes (section IV, B) and the catalytic transformations of adsorbed molecules under controlled atmosphere which is necessary for observing reactive intermediates and understanding mechanisms (section V). The differences between in-situ (NMR of adsorbed phase) and ex-situ (gas chromatography of products) analyses gives a direct observation of shape selectivity effects, which if present usually govern the overall process. Objectives b and c can be addressed using a combination of: NMR and reactor test studies, 3-dimensional x-ray diffraction structures and computer modelling of adsorbate-adsorbent interactions (theoretical chemistry). The crystalline nature of zeolites allows a detailed assessment of diffusivity and shape-selectivity effects. Pore systems can select (by size and shape) the passage of molecules in or out of the catalyst and the types of intermediates (and transition states) which can form [5, 6]. Competitive adsorption at the active site [7] is an important rate-controlling phenomenon which can be assessed by NMR studies and/or adsorption enthalpies.

Hydrocarbon transformations over acid zeolites is the main focus here. All of the atoms potentially involved in these reactions have active NMR nuclei (e.g. ^{1}H, ^{13}C, ^{17}O, ^{27}Al, ^{29}Si). Many types of NMR exper-

iments are possible with new ones being continuously devised. The application of in-situ NMR under the actual conditions occurring during the catalytic reaction (temperature, pressure, reagent mixtures, flow) is a formidable challenge. This is especially true when it is realized that NMR experiments giving high resolution usually require high sample spinning rates (10,000 revolutions per second).

NMR studies of zeolites, and their catalytic reactions, have been thoroughly reviewed in books published in 1987 [8] and 1994 [5]. Other less exhaustive reviews, dealing principally with zeolite structure, are also available [3, 9–11]. This review deals with the latest progress in the field and attempts to give an overview of which kinds of NMR studies (of the numerous possible varieties) are useful for investigating a particular phenomenon. Only the topics required for understanding catalysis are emphasized. For example, characterization of zeolites concentrates on the active sites not the gross structure. Future directions and prospects are also considered.

II. IN-SITU SOLID STATE NMR

A. Broadening interactions and MAS

The catalytic systems under study are heterogeneous: liquids adsorbed on solids. NMR characterization of solids is technically more demanding than for liquids, since in solids some interactions are not averaged out by molecular motion (causing larger spectral linewidths for solids). Stated very briefly, there are three solid state interactions which cause spectral broadening. Analysis of the broadening provides detailed information on the chemical nature and local structure of the nucleus under study. Usually only one type of interaction is dominant for a particular nucleus: magnetic dipole-dipole coupling (^{1}H), chemical shift anisotropy (^{13}C, ^{31}P) and quadrupolar coupling (^{2}H, ^{17}O, ^{27}Al). The first two interactions can be averaged out (if desired) by rapidly spinning the sample under MAS conditions (discussed below). The quadrupolar interaction is considered in section IV.A.3.a.

Organic molecules *strongly* adsorbed (chemisorbed) to the catalyst surface are not detected by solution state NMR methods. Strong chemisorption, of hydrocarbons on catalysts, usually occurs only at very low

adsorbate concentrations. On the contrary, hydrocarbons physisorbed at ambient temperatures on zeolites are usually liquid-like as far as molecular motion is concerned. However, for physisorbed molecules there is a typically a distribution of molecular species present on the solid surface, which requires high resolution conditions and/or other NMR methods (see section V.A.).

In order to increase spectral resolution in solids, a technique called **MAS** is used. Rapid sample rotation about an axis ca. 54.74° ("magic angle") with respect to the external magnetic field is able to average out dipolar interactions (which are angle dependent) while retaining isotropic chemical shift information [8, 12, 13]. This method gives high resolution spectra if the spinning frequency equals or exceeds the dipolar linewidth of the static sample. Today 14 kHz MAS rates are routine, which usually remove most of the dipolar broadening and leave only small spinning side-bands.

B. Sample preparation

Probably the reader is already pondering how in-situ studies can be made with the sample undergoing rapid MAS. What is needed is the capability of delivering gaseous reagents to the activated (dried) catalyst combined with NMR study under controlled conditions of atmosphere and temperature. Ingenious devices and protocols have been developed recently to address this problem [5, 14], including MAS samples under reagent flow conditions [15–21].

A typical solution for studying chemical transformations of adsorbate molecules in batch mode (without flow), is to prepare the dosed sample via vacuum line techniques in a small glass ampule [5, 14, 22]. The ampule, which fits snugly into the cylindrical MAS rotor, is then flame sealed with a glass blower's torch while being maintained at a temperature low enough to exclude any chemical reactions. The sealed ampule is then transferred to the NMR probe pre-equilibrated at a temperature low enough to preclude any chemical reactions. Sample heating, to cause reaction, can be performed within the probe or off-line. The ampule must be symmetrical along its long axis to perform MAS. Also the sample is small and care must be taken not to heat the reagents on the catalyst during sealing. A special device to prepare the sample at cryogenic temperatures was devised [5, 14, 22]. These difficulties can

be circumvented in some cases (e.g for reactions which occur at high temperatures) by transferring the dosed catalyst sample from the ampule to the rotor inside the inert atmosphere of a dry box. Once the cap is "glued on" the MAS rotor is air-tight.

III. SOLID ACIDITY

Solid catalyst acidity is, not surprisingly, far more complex than acidity in liquids. A complete description of it requires knowledge of both the density (concentration) and strength(s) (e.g. deprotonation energy) of the acid sites. Acidity in solids is widely studied and just beginning to be understood [4, 23–25], and NMR, studies have played an important role. For recent reviews see references [26–31]. Bronsted type acidity (proton donor) has been the main focus.

Analogies between solution (homogeneous) and solid state (heterogeneous) catalysis are difficult to make. The energetics of protonation is very different in zeolites compared to acid solutions [32]. And the solid interface imposes determining constraints on the chemical reactions occurring over it. No unified acidity scale for liquids and solids exists.

A. Nature of acid sites

There are three types of adsorption sites in acid zeolites (H form): non-acidic silanols SiOH, acidic bridging hydroxyls SiO(H)Al, and weakly acidic Lewis acids (electron-pair acceptors) thought to be due to tricoordinated Al or Si^+ (arising from dislodged Al).

The Bronsted acidity (proton donor) of the bridging hydroxyl is required to catalyze many hydrocarbon reactions. Compared to a normal silanol, the higher acidity of the bridging hydroxyl results from the formation of an additional bond from oxygen (Lewis base) to aluminum (Lewis acid). A lengthening of the O-H bond must accompany the formation of the third bond to oxygen according to Gutman's rule [4]. The bridging hydroxyl (Fig. 2) is usually depicted as structure I [4, 33] with the donor-acceptor bond as a dotted line and no formal charges. However, inclusion of the charges (II), for drawing an equilibrium with the dissociated form (III), is more analogous to solution state reactions ($H_3O^+ \leftrightarrow H^+ + H_2O$).

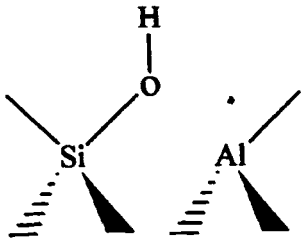

(I)

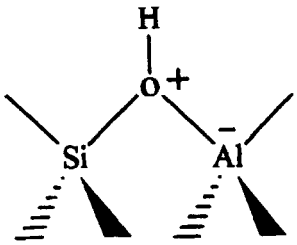

(II)

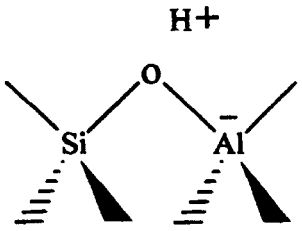

(III)

FIGURE 2 Equivalent formulas for representing the Bronsted acid site of a bridging hydroxyl group in an H form zeolite. The proton can be associated with any of the four oxygen atoms in the AlO_4^- tetrahedron

Quantum chemical studies place the proton bound directly to the oxygen [34] and predict relatively high proton mobility by jumping to the oxygen atom of any other AlO_4 tetrahedron [33].

Several experimental methods, used to characterize the **bridging hydroxyls** in zeolites, provide physical evidence for supporting the structures drawn above and for understanding the reactivity and accessibility of the acid site.

- Equal concentrations of framework aluminum and acidic protons were found by ^1H MAS NMR [35].
- The O-H bond is longer (more acidic) than for a silanol, since the IR stretching frequency is 100 to 200 cm^{-1} lower [34] and the ^1H NMR chemical shift is higher [5, 8 10].
- The bridging OH is pyramidal (not planar) and the oxygen has hybridization closer to sp^3 than sp^2, via ^2H NMR of SiO(D)Al groups [36].
- The acidic proton of H-Y is located at the site with the lowest Si-O-Al angle (ca. 141°), as found by high resolution neutron diffraction [37].
- The Al-H distance in H-ZSM-5, determined by ^1H MAS NMR, is 0.248 nm [35]. This distance increases (from 0.23 to 0.25 nm) with the size of the oxygen ring [30, 38].
- The proton is not "fixed" at one Al-O-Si site but mobile, as found by variable temperature ^1H [30, 31, 39] and ^2H NMR [29, 36].

Lewis acidity due to extra-framework aluminum species are generated during post-synthesis treatments (calcination, cation exchange, de-alumination) [40, 41]. Framework Lewis sites might also exist [42]. The role of Lewis acid sites in reactions is not yet well understood.

B. Acid strength

While it is known that the aluminum content and the local structure (of the acid site) greatly influence acidity, it is not yet possible to predict the Bronsted acid strength of a zeolite based on its structure. Two physical properties are important: electrostatics (charge compensation of framework Al) and lattice relaxation (changes in bonding affecting forces on

lattice atoms). A direct determination of molecular structure (atom positions) by XRD is not straightforward, since protons are invisible and analysis under in-situ conditions is very difficult. New double resonance NMR methods (see below) can give internuclear distances of selected nuclei (e.g. Al-H, Al-C) under in-situ conditions.

The most fundamental measure of Bronsted acid strength is the deprotonation energy for transferring the bridging hydroxyl proton to a base. This measurement is very difficult to realize experimentally, and evermore sophisticated theoretical quantum mechanical methods are being applied to estimate the energy [24, 33, 43].

The acid strength of a hydroxyl is reflected not only by the polarization of the O-H bond but also by the *polarizability*, which is manifested *only* in the presence of a base (proton acceptor). Without a base nearby (and no protonic solvent), acidity is not intrinsically defined. In fact, the relative strengths of acids are usually determined by comparing the extent to which they protonate the same base (or indicator). However, there are many inherent problems involved with ranking solid acidity using reference bases as probes [4, 32]. Solids are non-Hammett acids [44].

The most commonly used method for determining acid strengths on solids TPD of ammonia or other bases [4, 23]. However, interpretation of the TPD curve in terms of different acid site types is not trivial. At present, NMR studies of selected adsorbed probe bases appear to be the most sensitive means (apart from catalytic reactions) for probing acid strength in zeolites. Numerous examples follow (section IV, B). NMR studies also offer the advantage of providing acid site quantification, and in some cases a discrimination of acid types (based on chemical shift), using the same probe molecule.

The traditional views of acidity overestimate the strength of zeolites and neglect the role of the solid framework [26]. Many factors can influence the degree of proton donation to an adsorbed base, such as the conformation of the base (which affects its basicity). It is generally held that a correlation exists between Bronsted acid strength and the rate of the reaction catalyzed by the zeolite. Acid-base reactions are normally preceded by the formation of an H-bonded complex between acid and base. Farcasiu maintains there is no general correlation between hydrogen bond strength and acid strength [45].

IV. NMR STUDIES OF ACID SITES

A. Direct characterization of acid sites (unloaded zeolites)

Direct characterization of acid sites is often complicated by the fact that only a small percentage of the nuclei present are of actual interest. The CP technique can partially overcome this problem. CP was orginally devised to enhance the sensitivity of low abundance (rare) spins (^{13}C, ^{15}N, ^{29}Si) utilizing the greater polarization of bonded (abundant) ^{1}H nuclei. CP is a double resonance technique and provides the resonant transfer of magnetization from one spin system to another [8, 46]. It enhances selectively *surface* nuclei with protons in their coordination shells (e.g. ^{1}H-^{29}Si), and as a consequence does not give quantitative spectra. Recently, CP has been extended to quadrupolar nuclei (see ^{27}Al below). The following sections are organized by NMR nucleus and are arranged in order of increasing experimental difficulty.

1. ^{29}Si NMR

The chemical shift range for silicates is from –60 to –120 ppm. In zeolites with high amounts of aluminum, the five different types of SiO_4 tetrahedra: Si(4Al), Si(3Al,1Si), Si(2Al,2Si), Si(1Al,3Si) and Si(4Si) can be quantified by ^{29}Si MAS NMR spectroscopy. This allows the Si/Al ratio of the lattice to be calculated directly [3, 5, 8]. The ranges of chemical shifts (ca. 5 ppm downfield shift per Al introduced) are characteristic of the composition of the first coordination sphere. Silicon nuclei at framework defects or on the external surface of the crystal will have hydroxyl groups. The signal of Si(1OH,3Si) is near -103 ppm which usually overlaps with the Si(1Al,3Si) signal [47]. Thus, in zeolites with low amounts of aluminum (Si/Al > 20) the positions of the silicon resonances in the highly siliceous form must be known well before attempting Si/Al calculations. Additionally, ^{1}H spin counting (via ^{1}H MAS NMR) can be used to determine the amount of silanols. Given the typically small crystal sizes (nm, high surface area and silanol content) and low aluminum contents of industrial catalysts, ^{27}Al NMR is the method of choice for determining the Si/Al framework ratio.

Highly siliceous zeolites give much narrower resonances than zeolites containing aluminum. The presence of aluminum causes lattice disorder [3, 5] and broader signals due to a superposition of signals from nuclei in slightly different environments (even though highly crystalline). Fyfe and co-workers have carefully synthesized [48] high quality large crystals of some completely siliceous zeolites. From the "ultra" high resolution MAS spectra of these zeolites, the numbers and occupancies of the crystallographically inequivalent Si tetrahedral sites can be determined. There is a direct relation with XRD structures [49]. A total of 22 distinct signals were resolved for the monoclinic form of ZSM-5 [50], which has 24 crystallographically distinct SiO_4 tetrahedra in the asymmetrical unit of the unit cell.

This high spectral resolution permits other types of NMR studies, such as the effects of temperature and adsorbed molecules on the lattice [5]. Also, 2D NMR experiments (INADEQUATE, COSY) providing through-bond ^{29}Si-^{29}Si connectivites have been demonstrated [5, 49, 51].

There are well-documented linear correlations between Si-O-Si bond angle and ^{29}Si chemical shift [8, 52]. This is straightforward for ^{29}Si but not for ^{27}Al and ^{17}O since the istropic shift is displaced by the second-order quadrupolar shift [53].

New insight into the complex events of silicalite synthesis, involving hydrothermal crystallization of a silicate gel in alkaline solution, has been recently provided by several groups using ^{29}Si solution state NMR spectroscopy [54–56]. Tetraalkylammonium cations determine which kinds of negatively charged silicalite species form during polycondensation. The tetrapropylammonium cation directs the aggregation process (to ultimately yield the MFI structure) in solution by acting as a bifunctional interface and favoring the sequential formation of the bicyclic pentamer, the pentacyclic octamer, and the tetracyclic undecamer [55, 56]. The SiO_2 surface grows curved around the hydrophobic alkyl chains of the cation with the hydrophilic hydroxyl groups pointing outward. Martens et al. suggest that structure direction and hydrolysis of the silicon source take place simultaneously around the cation [56]. Smaller tetraalkylammonium cations give smaller cagelike structures. These studies reveal a far different role, more than just "templating", for the quaternary ammonium cations and provide fundamental knowledge useful for synthesizing new microporous systems.

2. $^1H/^2H$ NMR

^1H MAS NMR is used for detecting Bronsted acid sites. This subject was recently reviewed by Hunger [30, 31]. The catalysts must be thoroughly dried and kept sealed away from any trace of humidity. If the sample is dehydrated, then the homogeneous line broadening caused by proton-proton dipolar interactions is small and well-resolved spectra are obtained with rapid MAS (spin rate ≥ 10 kHz). There is no need to apply the more difficult method of CRAMPS [5, 31].

The ^1H NMR shift ranges for the various types of hydroxyl groups present in zeolites are well known [10, 29, 30, 57, 58].

1.2 to 2.2 ppm	isolated, non-acidic (SiOH)
2.1 to 3.0 ppm	H-bonded, non-acidic (SiOH)
3.8 to 5.2 ppm	bridging OH groups, acidic (AlO(H)Si)
5.2 to 7.0 ppm	disturbed bridging OH groups, acidic
ca. 10 ppm	H-bond between defect sites (SiO^---H--OSi), [59]
10 to 13 ppm	hydroxonium ions, acidic (H_3O^+)

Deconvolution of spectra into different peaks gives the amounts of each proton type. By using an external reference, with known proton content, the absolute quantities of each type can be found. IR characterization can corroborate the resolution of different hydroxyl types since there is a linear correlation between ^1H NMR chemical shift and the IR stretching vibration frequency, IR wavenumber (cm^{-1}) = 3884 – 68 x ^1H shift (ppm), [31, 60]. Also, IR absorptions are not affected by chemical exchange phenomena (very short timescale), unlike NMR which averages fast exchange processes.

^1H MAS NMR of dehydrated acidic zeolites gives several types of information [10, 30, 31].

acid strength	NMR chemical shift (more acidic = higher shift)
acid density	NMR signal intensity (number of sites)
H-Al distance	computer simulation of NMR spinning side-band patterns
OH mobility	NMR relaxation times

It should be stressed that a high ^1H shift results from both acidic *and* H-bonded protons. Adsorption of probe molecules (next section) can provide discrimination. NMR investigations of hydrogen bonds in zeolites and other solids were reviewed [61]. The structures of hydrogen bonds (determined by neutron diffraction) are linearly correlated with the isotropic ^1H chemical shift and the quadrupolar coupling constant of deuterium. Both of these NMR observables are related to bond polarization energy and the H-bond distance.

The mobility of acidic Bronsted protons in zeolites can be measured by variable temperature ^1H MAS NMR [30, 39, 62]. A high-temperature NMR probe (to ca. 350°C) is required. At elevated temperatures, protons jump between oxygens surrounding the aluminum atom causing a decrease in the spinning side-bands. The presence of spinning side-bands means that the jump frequency is small compared to the rotation frequency. The activation energy for proton mobility, estimated from the spinning side-band pattern, increases for less acidic protons. It increased from 45 to 61 kJ/mol for H-ZSM-5 and H-Y, respectively [39]. Proton mobility in H-MOR increased with increasing Si/Al ratio [62], as expected for an increase in acidity.

Deuterium exchange of the bridging hydroxyl allows detailed investigation of the O-D bond using the nuclear quadrupole interaction (see next section). Wideline (non-spinning) ^2H NMR revealed the non-planarity of the bridging hydroxyl in H-form zeolites [36]. Much longer accumulation times are required compared to ^1H, even with isotopic exchange, due to the very large linewidths. The mobilities of the acidic deuterons in zeolites are clearly evidenced as the motional averaging of the quadrupolar broadening interaction (as for ^1H, mentioned above, but where the interaction was ^1H-^1H dipole). The quadrupolar interaction of deuterium in the SiO(D)Al group increases (less mobile) with an increase in the framework aluminum content due to a decrease in acid strength [29].

3. ^{27}Al NMR

The acid sites of zeolites (Bronsted and Lewis) are associated with aluminum. Accurate quantification of *framework aluminum* (not possible by elemental analysis) is fundamental for exploring the relationship between Al content and catalytic activity. In general, the acid strength increases with decreasing Al content.

For these reasons, ^{27}Al MAS NMR is an important tool for zeolite study. Applied correctly, it can quantify the various aluminum types, such as in framework positions with Td coordination (AlO_4, isotropic shift 40 to 60 ppm) and in non-framework positions with Oh coordination (AlO_6, ca. 0 ppm).

a. Quadrupolar broadening

One advantage of studying quadrupolar nuclei (e.g. ^{2}H, ^{17}O, ^{27}Al) is that their solid state spectra are influenced mainly by the local environment around the nucleus, and not the long-range dipolar effects often encountered in solid state ^{1}H NMR studies.

The main complication in performing ^{27}Al NMR stems from spectral broadening due to the quadrupolar nature of this isotope (spin quantum number, I = 5/2,). Nuclei with spin quantum numbers (I) ≥ 1 exhibit an electric quadrupole moment (eQ) in addition to the magnetic dipole moment. Interaction of this quadrupole moment with the electric field gradient (eq), due to non-spherical charge distribution, surrounding the nucleus broadens the solid state lineshape. The QCC is a measure of the strength of this interaction ($QCC = e^2qQ/h$) and can be calculated by simulation of the NMR lineshape [13]. The QCC is a sensitive function of the geometry and coordination symmetry about the ^{27}Al nucleus [31, 53]. In general, lower symmetry gives a greater QCC and thus a larger linewidth. An empirical linear correlation between QCC and the deviation from ideal tetrahedral coordination (O-Al-O angle = 109.5°) was found for minerals without acid centers [63]. Koller et al. concluded that geometrical strain is not sufficient for explaining the QCC values in H^+-zeolites [64]. They found that the QCC correlates with the Al-O bond perturbation (electronic bond strain).

b. Detection by MAS NMR

The most common approach for ^{27}Al has been to perform MAS NMR and selectively observe the strong central transition (+1/2,-1/2), which is unaffected by first-order quadrupolar effects. However, for very large QCC (i.e. MHz) the contribution of second-order quadrupolar broadening to this transition is so great that MAS is useless.

Framework Al nuclei in *dehydrated* H-form zeolites have the largest QCC (11–18 MHz) known for ^{27}Al [29, 64, 65]. They are severely distorted AlO_4 tetrahedra. Their signals are broadened beyond detection

(invisible) using standard pulsed MAS NMR methods [53] at low magnetic fields (7 T or less). Even "tal quale" forms (partially hydrated) of H-zeolites have considerable amounts of undetectable ^{27}Al signals. For this reason, absolute quantification of the total aluminum is advisable. This is done by comparing the spectral areas with a standard having a low QCC (i.e. high coordination symmetry, Td). This proves critical when trying to rationalize acidity based on Td/Oh Al ratios.

One simple solution to obtaining high resolution MAS spectra with no, or reduced, ^{27}Al quadrupolar effects is to decrease the QCC by adsorbing water. The presence of a chemisorbed hydroxonium ion (and other adsorbed bases, next section) "relaxes" the distorted Al coordination symmetry [31, 66] and the electronic Al-O bond strain [64] of dehydrated H form zeolites.

Apart from causing detection problems, quadrupolar effects can also complicate spectral interpretation. The intensities, shapes and positions of NMR lines in the central transition (+1/2,-1/2) spectrum, occurring from 0 to 60 ppm, are affected by the quadrupolar interaction. Quantification of aluminum types by spectral deconvolution of this region is not usually possible since these signals are asymmetric, due to distributions of second-order quadrupolar effects. Samoson reported an ingenious solution to this problem in 1985 using (±3/2, ±1/2) satellite transition sideband spectra [67]. In contrast to the central transition, the satellite transition is strongly affected by the first-order quadrupolar interaction. This interaction greatly exceeds MAS speeds giving numerous spinning sidebands. The signals making up the inner spinning sidebands of the first satellite transition (±3/2 ↔ ±1/2) are symmetric and can be used to obtain the relative Al amounts. Jager reviewed satellite transition spectroscopy of quadrupolar nuclei [68]. This method was used to determine precise isotropic shifts and reveal a linear relationship between ^{27}Al isotropic chemical shifts and the mean Al-O-Si bond angle of zeolites [69].

c. Double resonance MAS NMR

Numerous types of double-resonance solid state ^{27}Al MAS NMR experiments have been devised to study aluminum nuclei located at the chemically most interesting, but spectroscopically least accessible, sites of catalysts.

The simplest example of a double resonance technique would be ^{27}Al observation with ^{1}H decoupling. In the case of zeolites, no discrimina-

tion of aluminum types is possible (quadrupolar interaction is much greater than the heteronuclear dipolar interaction). However, if the radiofrequency irradiations are made simultaneously at power levels which fulfill the Hartmann-Hahn condition, then thermal contact between the two spin systems is made (CP) and the resonances of aluminum nuclei with protons bonded nearby are enhanced. Thus, CP allows assignment of through-bond connected nuclei (see above). CP from protons to aluminum ($^{1}H \rightarrow ^{27}Al$) has been applied to zeolites [70, 71]. It has even been demonstrated for two quadrupolar nuclei such as $^{27}Al \rightarrow ^{17}O$ [72].

^{1}H-^{27}Al SEDOR was used to identify protons close to the ^{27}Al site [73] and to measure the internuclear H-Al distance [74]. Dipolar recoupling techniques have been designed to *restore* the dipolar couplings to solid state spectra which were averaged out by MAS (necessary for high resolution). These techniques can provide accurate distances (up to 0.5 nm) between spin pairs [75]. Originally applied to biological systems, they are being extended to zeolites. Fyfe and co-workers demonstrated the feasibility of ^{27}Al-^{29}Si dipolar recoupling experiments in zeolites [76]. Grey and Vega devised the ^{1}H-^{27}Al TRAPDOR (transfer of populations in double resonance) experiment to determine the QCC of ^{27}Al nuclei coupled to protons with high accuracy [65]. TRAPDOR allows the study of aluminum species with large QCC and their nearby proton nuclei [41].

Double resonance methods, which establish through-bond dipolar connections between two different nuclei, have great potential for making spectral assignments (e.g. ^{1}H-^{27}Al, ^{17}O-^{27}Al). Many different scenarios for such experiments, including extension to triple resonance and/or addition of adsorbate molecules (see next section), can be envisioned and significant advances are expected in the future. Recently, van Wullen reported triple resonance ^{1}H-^{13}C-^{27}Al TRAPDOR measurements for detecting ^{13}C-^{27}Al proximities in solids [77].

d. MQ-MAS NMR detection

This is a new two-dimensional solid state NMR method to give line narrowing of the central transition of a quadrupolar nucleus by changing the coherence state of the observed spins. Nuclear transitions other than the central one (+1/2,-1/2) in the multi-level spin manifold are excited and monitored. Second-order quadrupolar effects are refocussed via MQ correlation. MQ-MAS is compatible with standard solid state NMR

spectrometers and gives highly resolved spectra, in one dimension, devoid of quadrupolar effects [78].

MQ-MAS NMR is the most significant development in solid state NMR of half-integer spin quadrupolar nuclei in the last 10 years. It was devised by Frydman and Harwood in 1995 [78] and subsequently developed, also by other groups, to provide: increased sensitivity by sampling the free induction decay during a train of selective refocussing pulses [79], increased resolution through z-filtering [80, 81], more rapid data collection using pulsed-field gradients instead of phase cycling of radio frequency pulses [49] and quantitative spectral intensities [81, 82]. MQ-MAS has been combined with CP [83] and with REDOR [84] to establish connectivites and internuclear distances between spin 1/2 nuclei (e.g. ^{1}H) and ^{27}Al nuclei.

^{27}Al MQ-MAS NMR was used to distinguish two framework AlO_4 sites in H-ZSM-5 and establish relations between ^{27}Al, ^{29}Si and ^{1}H NMR data [85].

e. Non-MAS methods of detection

The technically demanding methods of double rotation and dynamic angle spinning [5, 86, 87], which employ sample spinning about more than one axis, will not be mentioned. Also, nutation spectroscopy (two-dimensional array of excitation spectra) is omitted [5, 69, 88].

The methods listed above circumvent in some way the large quadrupolar effects on ^{27}Al signals. But there are superconducting magnets which permit the fields to be swept. This allows recovery of even the broadest ^{27}Al lines [89, 90].

High magnetic field strengths (minimum 11.7 Tesla, 500 MHz for ^{1}H) allow observation of nuclei with large QCC using the echo Fourier technique [29]. High field solid state NMR spectrometers have recently become commerically available (e.g. 18.8 T, ^{1}H freq.= 800 MHz) [58, 91].

4. ^{17}O NMR

The very low natural abundance of ^{17}O (0.037%) usually requires isotope enrichment. This nucleus should be important for studying lattice structures. The ^{17}O spectra of zeolites can be deconvoluted into two components (Si-O-Si, Si-O-Al), permitting a calculation of the framework Si/Al ratio [92]. MQ-MAS is also a very important development

for this quadrupolar nucleus (I = 5/2), which also has large QCCs in zeolites. It was recently applied to study an aluminosilicate glass [93] and a natural zeolite [94]. A correlation between ^{17}O isotropic chemical shifts and mean Si-O-Al bond angles in zeolites was found using this technique [95].

B. Characterization of acid sites using basic probe molecules

The problem of detecting selectively the nuclei of interest with high sensitivity (encountered in the direct method above) can be avoided by addition of gaseous probe molecules, with ideal NMR and acid/base properties, to dehydrated catalysts. Weakly basic probes can be used to titrate acid sites. Titration is facilitated if the probes are gaseous. Strongly basic probe molecules can chemisorb irreversibly and be considered a poison. More practically, the molecules of actual catalytic interest (hydrocarbons) can be used.

A large number of articles, utilizing different probes, concern evaluation of Bronsted acid-base interactions. This, in itself, demonstrates that no single method is generally accepted. Some workers even question the usefulness of basic probe molecules. Most studies with probe molecules are made to distinguish/quantify the different types of acid sites. As will be emphasized below, acid strength is more problematic to determine. Apart from strength, also the quantification of acid sites is not always straightforward, especially when cross-polarization is required or when the probe molecule exchanges rapidly between different adsorption sites.

Double and triple resonance methods (e.g. ^{13}C-^{27}Al, ^{1}H-^{15}N-^{27}Al), along with recently developed recoupling experiments, provide connectivites between selected nuclei. They are principally used to aid spectral interpretation (e.g. assigning which aluminum nucleus is bound to an adsorbate), which facilitates quantification of the acid sites (concentration). Recoupling experiments determine inter-nuclear distances, information useful for interpreting acid strength in terms of adsorbate-acid site structure.

1. Chemical shifts

a. Water

Probably the simplest example of a probe is water, a small molecule and weak "hard" base. Adsorption of H_2O at the bridging hydroxyl in zeo-

lites has been studied in detail to elucidate exactly how proton transfer occurs. Is the adsorbate complex ionic (proton transfer) or neutral (H-bonded)? This problem will be addressed in section V.

Acidic protons have low field shifts. But, as stated above, so do H-bonded protons. The use of ^1H NMR shifts to measure acidity, near ambient temperatures, is thwarted by chemical exchange processes. This problem was solved by making spectra at low temperaure. Broad-line ^1H NMR at 4K is a new method (using non-spinning samples) providing accurate Brönsted acidity measurements in solids [96, 97]. At this low temperature hydrogen atoms do not undergo rapid chemical exchange and the concentrations of all the hydrogen-containing species (H_3O^+, $H_2O\cdots HO$, H_2O, OH) can be determined. When the number of water molecules is the same order of number as the Bronsted acid sites, the chemical interaction can reveal the intrinsic acid strength. An acidity scale was determined. The concentration of H_3O^+ ions increases with water loading until the number of water molecules equals the number of initial SiO(H)Al groups. This does not appear to be true for dealuminated zeolites (with extra-framework Al), where the concentration increases continuously with loading.

Farcasiu has questioned the applicability of water as an indicator of acid strength after finding that the basicity of water is strongly dependent on the type of acid used [98].

b. Ketones

Changes in ^{13}C chemical shifts of organic molecules such as ketones have been used to rank the acidities of strong acid catalysts [44, 99, 100]. ^{13}C NMR shifts of carbonyls are very sensitive to protonation equilibria.

Farcasiu and co-workers found that the unsaturated ketone mesityl oxide (4-methyl-3-penten-2-one) is a particuarly good choice since the signals of the C3 and C4 carbons move upfield and downfield, respectively, on protonation. Full protonation causes a large change (ca. 50 ppm) in the shift of the C4 signal, demonstrating that C4 carries a significant fraction of the positive charge. The difference in chemical shifts for these two signals ($\Delta\delta$) provides an acidity-dependent pararmeter (degree of protonation) which is independent of medium effects. Relative acidity based on the shift of only one nucleus in a molecule is susceptible to medium effects. The $\Delta\delta$ parameter was correlated with the

H_0 values for sulfuric acid solutions. The acidity function of sulfuric acid (H_0 = -log hydrogen ion activity), determined using Hammett indicators and UV-visible spectroscopy, was used to calibrate $\Delta\delta$ since it is the best known of any strong acid (pure acid $H_0 = -12.0$). The $\Delta\delta$ values of mesityl oxide were used to calculate H_0 for other acids, including solids [44, 99]. Application of this technique, for comparing liquid and solid acidity, is of great practical interest.

A study of acid zeolites, using $\Delta\delta$ of mesityl oxide, ruled out the idea that zeolites are superacids [100]. At 25°C, H-ZSM-5 (Si/Al = 19, the most acidic zeolite studied) is only as strong as 70% sulfuric acid ($H_0 = -6.4$).

c. Acetonitrile

The main problem with ketones is that they decompose or oligomerize at higher temperatures. Ideally, acidity should be measured at the temperature of catalytic application. For this reason Haw and co-workers selected acetonitrile [101]. It is unreactive, toward side reactions, up to 350°C. A large (reversible) downfield shift of the nitrile carbon resonance was observed on raising the temperature of loaded zeolites (H-Y, H-ZSM-5). It is known, from Olah's work [102], that full protonation of acetonitrile in magic acid (FSO_3H/SbF_5) solution causes a 10 ppm upfield ^{13}C shift. Thus, in solution the nitrogen is positively charged ($H_3C\text{-}C{\equiv}N^{+}\text{-}H$). The downfield shift in zeolites [101] was interpreted as a progressive proton transfer, with increasing temperature, to give a partial positive charge on the nitrile carbon ($H_3C\text{-}C^{+}{=}N\text{-}H$). Ab initio calculations revealed that only bent structures of hydrogen-bonded acetonitrile account for the NMR shifts. The bent structure, formed at higher temperatures, is more basic. As these authors rightly emphasize, changes in the structure of the base (not possible in solution) can enhance zeolite acidity [101]. The confinement of a weak base near the acid site, imposed by the pore structure, is an important aspect of catalysis which is often overlooked. By this method, the Brönsted acidity of H-β, measured up to 250°C, is intermediate between that of H-ZSM-5 and H-Y [73].

The conculsions of Haw [101] regarding the species formed in zeolites have been challenged by Sepa et al. on the basis of IR work [103]. No evidence was found for a change in the C-N bond order, ruling out the formation of any C=N containing species. They suggest that dynam-

ical processes, rather than a chemical change, are responsible for the observed ^{13}C NMR shifts.

d. Miscellaneous organic bases

Bosacek et al. adsorbed CH_3I on Na-zeolites and used the ^{1}H and ^{13}C signals of the methoxy groups formed to characterize lattice oxygens [104]. Methoxy groups form on strong acid sites at low temperature (25°C), and also on weak acid such as silanols at higher temperaures (300°C). The ^{13}C NMR shift of the chemisorbed methoxy group increases with increasing electronegativity of the attached oxygen.

Adsorption of weak bases, such as C_2Cl_4, induces downfield ^{1}H NMR shifts of surface hydroxyl group signals which reflect acid strength, since the deprotonation energies of the hydroxyl groups can be calculated [105, 106].

Other types of basic probe molecules have been used in NMR spectroscopic studies of zeolite acidity [8, 10]: ^{13}C NMR of CO, ^{15}N NMR of pyridine [107], NH_3 [108] and N_2O [109], ^{19}F NMR of *p*-fluoroacetophenone [110] and ^{31}P NMR of $P(CH_3)_3$ [111–113], $P(OCH_3)_3$ [114] and $P(OC_2H_5)_3$ [115]. The shifts of these molecules, in *slow* chemical exchange between various sites, reveal if they are chemisorbed at Lewis or Bronsted acid sites. (Probes such as N_2O and CO exchange too rapidly). Quantities of sites are usually determined from signal areas using low probe molecule concentrations to avoid difficulties ("apparent" shifts and intensities) due to chemical exchange.

The difference in ^{31}P shift for the chemi- and physi-sorbed forms of $P(OC_2H_5)_3$ was claimed to provide a relative acidity scale [115]. Assignments of ^{31}P signals are facilitated by ^{1}H-^{31}P-^{27}Al triple resonance NMR methods [113]. The size of the probe molecule is important since acid sites may be located in pores with openings too small to allow interaction (e.g. fluroacetophenone). Desorption experiments can be carried out at higher temperatures to give information on relative strengths (as commonly done with IR).

Lunsford and co-workers studied $P(CH_3)_3$ adsorbed in zeolites and found the scalar coupling constant between phosphorus and hydrogen ($J_{P\text{-}H}$) to be a more sensitive indicator of Bronsted acid strength than the chemical shift [112]. The variation in J coupling magnitude may reflect the distance between the protonated adduct and the negatively charged framework.

Grey and co-workers applied the ^{27}Al-^{31}P INEPT experiment to probe the interaction between $P(CH_3)_3$ and Lewis acid sites in zeolites [116].

2. Deuterium exchange

^1H NMR analysis made after adding ^2H_2O (D_2O), or other deuterated bases (e.g. methanol, pyridine [31], can identify *which* sites react more readily and, thus, have greater acid strength. In this case, the disappearance of ^1H signal, via facile proton-deuterium exchange ^1H-^2H exchange reactions) shows which hydroxyl groups are involved. This can be used to study the locations of hydroxyl protons [30].

H-D exchange between the acidic hydroxyl proton and deuterated benzene can be observed at 25°C for zeolites. The rate of this simple substitution reaction provides a dynamic measure of Bronsted acidity. Experimentally, the time-dependent growth of the ^1H MAS NMR signal for benzene (at 7 ppm) can be monitored after jumping the sample to the desired temperature [117, 118]. These kinetic measurements, as a function of temperature [117], confirmed again (e.g. ^1H mobility above) that H-ZSM-5 has greater acid strength than H-Y (activation energies of 14 and 25 kcal/mol, respectively). Laser-heated temperature jump methods allow characterization of relatively fast exchange rates (10 min^{-1}). Mildner and Freude measured exchange rates up to 300°C with this method [118], and for the highest rates (100 min^{-1}) 2D-NOESY of normal benzene (at dynamic equilibrium) was used to calculate the rate.

3. Catalytic activity

Test reactions of hydrocarbons are commonly used to control the quality of industrial catalysts. Rates of reactions such as i) alcohol dehydration, ii) olefin isomerization, iii) alkane isomerization and cracking, and iv) isomerization and disproportionation of alkylaromatics are used to evaluate the strength of acid sites [119]. These reactions are usually monitored by gas chromatographic analysis of the products flowing off the catalyst. Greater information is available if the interactions and reactions of probe molecules are determined in situ. These studies offer a measure of "effective acidity" under the real reaction conditions.

In-situ studies of 1-butene double bond isomerization are useful for evaluating catalyst acidity [8, 120, 121]. The kinetics of these first-order

reactions can be followed by ^{13}C NMR at temperatures giving convenient half-lives. In the case of eolites, low temperatures (e.g. – 50°C) are needed and the competing oligomerization side reaction complicates rate determinations.

4. Molecular dynamics

The dynamic behavior of probe molecules can yield information on the active sites (in addition to subtleties of the internal pore structure). This approach, which can be combined with rapidly evolving computer studies (molecular modelling), has been scarcely utilized. Here again, many NMR methods developed for biomolecules and organic polymers are being extended to small molecules adsorbed in zeolites. Note that the term "dynamics" refers to molecular motions (e.g. overall tumbling), but it also includes chemical or conformational exchange phenomena. NMR is unique in its ability to study chemical exchange in systems at dynamic equilibrium. Other methods (e.g. stopped flow, temperature jump) monitor the kinetics of the return to equilibrium.

A variety of NMR methods can be used to study the dynamics of molecules adsorbed at catalytic surfaces [122, 123]: relaxation studies, lineshape (static and spinning) simulations, spin-population labeling and multi-dimensional exchange NMR. Within a reasonable temperature range, any dynamic molecular process will have a time constant compatible with one of these methods. If multiple dynamic processes occur simultaneously, the two-dimensional versions of these methods are highly advantageous for resolving the different processes.

a. Relaxation studies

Relaxation studies cover the fastest frequency motions (10^{11}-10^4 s^{-1}) and involve measuring the rate of energy exchange between nuclei and their environments. Longitudinal relaxation is sensitive to MHz frequency motions, such as overall molecular rotation. Auerbach et al. used ^2H longitudinal (spin-lattice) relaxation to study perdeuterated benzene mobility in Na-X and Na-Y [124]. They found that benzene moves much more rapidly in Na-X than in Na-Y due to greater intercage hopping rates.

Chen et. al used ^2H longitudinal relaxation and DQF ^2H NMR to study benzene in Y zeolite [125]. The adsorbate was found to exchange

between two motional forms (isotropic and anisotropic) which cannot be observable using normal (single quantum) spectra. They stressed that this exchange process, and the molecular distribution within the pore system resulting from it (see section V.A.2), must be considered when interpreting relaxation data.

A cross-relaxation experiment called 2D ^{1}H NOESY, indispensible for solution state studies, was used to calculate the mean reorientation time (6.1×10^{-9} s) for the allyl group of allyl alcohol adsorbed in Na-X at 27°C [126]. ^{13}C T_1-rho relaxation measurements (longitudinal relaxation in the rotating frame) provide information on molecular motions in the kHz regime for solid organic molecules [127].

b. Line shape simulations

Line broadening due to anisotropic effects (chemical shift, ^{13}C or quadrupolar, ^{2}H) constitutes a sensitive means for characterizing dynamics since molecular motions will cause line narrowing. Simulation of solid state lineshapes yields the frequency and type of molecular reorientation, if the lineshape for the completely rigid system is known. Analysis of static (low resolution) lineshapes usually requires isotopic labeling to distinguish functional groups. Alternatively, the spectral resolution can be increased with MAS and the spinning sideband pattern can be exploited.

Rotational motions over a wide range of frequencies (10^{7}-1 Hz) can be monitored [128, 129]. Workers have investigated the dynamics of benzene adsorbates in Na-Y [130], methylamines in H-Y [131], and dimethyl ether in zeolite H-RHO [122] using this method (deuterated adsorbates) and solid state ^{2}H NMR. Harris and co-workers pointed out that different dynamical models for re-orientation of benzene, about an axis perpendicular to the molecular plane, may fit the same experimental data [132]. The method has limitations for distinguishing the correct dynamic model. The ^{13}C lineshapes of CO_2 adsorbed on the mordenite zeolite revealed a rigid linear molecule at lowest coverages. At intermediate coverages it rotates about an axis perpendicular to the O=C=O bond and at high loadings undergoes isotropic motion typical of physisorbed species [122].

Variable temperature lineshape analysis [13] probes the intermediate motional regime (10^{7}-10^{3} s^{-1}) of chemical exchange for liquid (isotropic) systems in dynamic equilibrium. The temperature must be varied

enough to observe the coalescence of distinct signals from the species in "fast" exchange. It was used to measure the rate of ether interchange with boron trifluoride complexes in solution. This provides a calibration of Lewis acidity based on the strength of interaction with diethyl ether as a probe base [133].

c. Spin-population labeling

Spin-population labeling and 2D exchange NMR techniques examine slow processes (10^{3}-10^{-2} s^{-1}). The former is analogous to isotopic labeling (but using radio frequency pulses), and the label has a certain lifetime. The exchange of CO between bridge- and linearly-bonded forms on Rh/silica was studied by this method [122].

d. Multi-dimensional exchange spectroscopy

2D exchange spectroscopy in solids was orginally proposed by Ernst et al. [134]. It is used to study slow exchange processes (lineshapes not affected by dynamics) between sites with resolved chemical shifts [135]. Off-diagonal cross peaks observed in the 2D spectrum indicate that an exchange process (during the mixing period) has transferred magnetization from one site to another. The nuclear magnetization is forced into a non-equilibrium state while the chemical species remain untouched in dynamic equilibrium. The exchange process may involve a re-orientational movement of a molecular segment or exchange between configurational or conformational isomers (since molecular orientation and conformation can effect a change in chemical shift).

Unlike the other NMR methods, this experiment yields molecular reorientation geometries and time scales without the need for a model of the motional process [123]. Spiess and co-workers have widely applied this 2D technique to ^{2}H and ^{13}C nuclei in solid polymers [129]. They developed a 3D DICO experiment (^{2}H NMR) which gives detailed information on the time scale and geometry of rotational processes for polymer chain segments simultaneously [136].

Exchange frequencies lower than 10^{-2} s^{-1} are not usually studied since *spectral* spin diffusion between nuclear spins becomes dominant. The static dipolar interaction between nuclear spins causes spin diffusion (propagation of Zeeman and dipolar order) by mutual spin flips [135]. Spin diffusion is strongly dependent on the inter-nuclear separation and for this reason has been widely used to study microscopic heterogeneity

in solids (see section V.A.) such as domain sizes in polymer blends [129].

5. Molecular self-diffusion

NMR is also used to study molecular transport in zeolites. The self-diffusion coefficients of adsorbed molecules can be measured directly by pulsed magnetic field gradient NMR [10]. The long-range translational movements of molecules (diffusion over μm) are detected, rather than the much shorter movements (e.g. molecular tumbling) which influence relaxation measurements. The rate of molecular transport (*intra*-crystalline) is sensitive to interactions with the pore walls, other adsorbed molecules, and the active site. The application of these methods to zeolites [137, 138] requires high-power (> 100 G/cm) pulsed field gradients and is limited since large crystals (>10 μm) are required to avoid restricted diffusion phenomena. The mean molecular displacements must be smaller than the crystallite diameters.

V. NMR STUDIES OF CATALYTIC HYDROCARBON REACTIONS

^{13}C MAS is the principal in-situ NMR method used to study reaction mechanisms. In situ is defined here as involving sealed samples with controlled atmospheres. There are several reviews on this topic [5, 8, 22]. The low natural abundance of the ^{13}C isotope (1%) usually requires ^{13}C labelled reagents. Isotopic labelling is advantageous since it reveals any scrambling reactions of carbon atoms. Recent in-situ NMR studies of heterogeneous acid catalyzed processes, listed below, involved mainly the H form of ZSM-5. Basic zeolites, those containing alkali metal cations, have received less attention.

In-situ NMR stidies before 1987 were reviewed by Engelhardt and Michel [8] and will not be discussed here. Haw provided a more recent review in 1994 [5]. The compromises made in experimental conditions of in-situ studies must be considered when making mechanistic conclusions. For example, the first reaction in this series (a redox one employing a non-zeolite catalyst), produces essentially all of the world's methanol supply. It is carried out at high pressure (50 bar). The in-situ study [139] was made at low pressures where methanol decomposition

is spontaneous. Thus, the focus was really on the reverse of synthesis. Syn gas is a mixture of CO, CO_2 and H_2.

Reaction	*Catalyst*	*Ref.*
syn gas to methanol	$Cu/ZnO/Al_2O_3$	[139]
methanol to gasoline	H-ZSM-5, H-OFF	[140–143]
methanol to light olefins	H-SAPO-34	[144, 145]
ethene oligomerization/ cracking	H-ZSM-5, H-Y, H-MOR	[138, 146–148]
ethene hydrogenation	RuH-Y	[149]
propane to butane	H-MFI	[150]
propane aromatization	GaH-ZSM-5	[22, 151]
propene oligomerization	H-Y	[16, 152, 153]
isopropanol reactions	H-Y, LaNa-Y, Na-X, Cs-X	[16, 137]
allyl alcohol to hydrocarbons	H-ZSM-5, H-Y	[154]
butyl alcohols to hydrocarbons	H-ZSM-5	[155, 156]
butene oligomerization	LaH-Y, CaNaH-Y	[8, 120]
isobutene oligomerization	H-ZSM-5, H-Y	[157, 153]
butadiene oligomerization	H-ZSM-5, H-Y	[158]
hexane reactions	PtK-L	[22, 159]
MTBE synthesis	H-β	[20]
heptane cracking	H-β	[160]
benzene isopiopylation	H-ZSM-11	[161, 22]
toluene alkylation	H-ZSM-11, NaKCs-X, NaCs-Y	[162–164]
ethylbenzene alkylation	H-MOR	[165]

Typical in-situ NMR experiments are made in batch (without flow) using low adsorbate concentrations. This facilitates the detection of intermediates (low steady state concentrations), otherwise obscured by excess reagent, and lessens intermolecular adsorbate reactions. Ideally, in-situ studies should be made at the real reaction conditions, such as those for a flow reactor. There is a continuing technological drive towards more realistic in-situ NMR conditions with MAS: high temperatures [5, 10], temperature jump using a laser [146, 166, 167], high pressures [168], and continuous reagent flow [15–21].

In-situ NMR studies without flow are different than the reactor in two important ways. There is no continuous removal of volatile products, and the contact times (between reagent and catalyst) are too long. Hunger and Horvath developed the means for making MAS NMR with flow in 1995 [15]. The catalyst bed, as a hollow cylinder in a 7 mm rotor, rotates at speeds up to 3 kHz around as fixed injection tube. The exhaust tube can be connected to an on-line gas chromatograph to provide simultaneous anlaysis (ex situ) of the products leaving the catalyst bed [19]. MAS flow NMR has since been implemented by other groups [17, 18, 21]. Maciel and co-workers combined regeant flow with a magic angle hopping apparatus. This is an alternative to MAS for line-narrowing, where the static sample is hopped by 120° about the magic angle [169].

Haw's group devised a pulse-quench reactor [143, 170, 171] to study mechanisms. The gas stream flowing over the catalyst bed is rapidly switched to cryogenically cooled nitrogen, with high speed valves under computer control, to provide a time resolution of 200 ms or less. The sample is then transferred to the MAS rotor in a glove box without exposure to the atmosphere.

A. Adsorbed molecule characterization

Any in-situ mechanistic study of hydrocarbon reactions requires characterization of the adsorbates to some extent. This usually means complete assignment of ^{1}H and/or ^{13}C spectra to provide the 2-dimensional structure. Methods to determine 3-dimensional structures (conformation) were mentioned above (under acidity). Given the numerous molecular forms typically encountered (reagents, intermediates, products), complete signal assignment is a considerable challenge. Various approaches are possible, including the solid state NMR versions of solution state methods so useful in organic chemistry.

1. Molecular structure

Strategic ^{13}C labeling of the reagents provides spectra without the signals arising from natural abundance positions. This, combined with solid state MAS NMR, is the most common method for unraveling the spectra of hydrocarbons. Mechanistic information, related to time

resolved molecular rearrangements, is obtained simultaneously. Complete deuterium labeling combined with ^1H NMR is another possibility. ^1H MAS NMR spectroscopy was used to monitor the concentration of fully deuterated adsorbate complexes and suface hydroxyls as a function of time [20].

Double and triple resonance techniques in solids have great potential for characterizing adsorbates in catalysts. SEDOR measures the dipolar interaction between selected unlike spins. It is valuable for making signal assignments and measuring internuclear distances [5]. ^1H-^{13}C SEDOR was used to reveal the formation of an ethylidene species on Pt clusters supported on alumina at low temperature [172]. Double resonance methods such as REDOR and TEDOR, that measure weak heteronuclear dipolar couplings in the presence of large chemical shift anisotropies, employ rotational echoes generated by MAS to give connectivity and distance information [75, 173].

Two-dimensional (2D) experiments increase the spectral resolution by correlating normal isotropic chemical shift information (F2 dimension) with some other NMR parameter along the second dimension (F1). 2D J-resolved ^{13}C NMR gives carbon multiplicities (number of attached protons per carbon) and the values of ^{13}C-^1H scalar coupling constants in the F1 dimension [5, 148].

Line broadening due to anisotropy provides a means for determining chemical shift tensors of ^{13}C nuclei. The angular distribution of of electron density, bond angles and bond distances are determined for a paticular ^{13}C nucleus by simulating spectra broadened by CSA. In cases of spectra with severe signal overlap, the CSA information can be contained in a second dimension. This experiment, devised by Gan [174], is MAT and involves slow sample spinning (30 Hz) and rotor synchronized rf pulses [175]. MAT was used to differentiate four different types of methoxy groups formed on ZSM-5 after adsorption of methanol [176].

Double quantum ^1H NMR can be applied to determine distances within and between functional groups in solids. Spiess and co-workers reported the means for analyzing the double quantum spectra to yield the structural information [177].

The 2D exchange ^{13}C NMR experiment (mentioned in section IV.B.4) was used to detect the coexistence of chemi- and physisorbed methanol intrinsic to the H-ZSM-5 structure [178]. In this case no correlations

(cross peaks) were found in the 2D spectra, ruling out chemical exchange (see section IV.B.4.d).

2. Molecular distribution

The distribution of hydrocarbon species within the intra-crystalline space of zeolites is another phenomenon which is readily addressed by NMR studies. Initial applications of spin-diffusion (or 2D-exchange, section IV.B.4.d) and multiple quantum spin counting methods have been reported.

"Spectral" ^{13}C spin diffusion was found to occur by both intra- and inter-molecular means in ZSM-5 zeolite depending on the size of the hydrocarbon used [179]. Intra-molecular spin diffusion dominates for larger molecules (hexane, heptane) since the linear channels impose a single-file arrangement and prohibit the molecules exchanging positions. Smaller molecules (propane, isobutane) exhibit inter-molecular spin diffusion between them since they are mixed at a microscopic level.

MQ NMR is a 2-D technique well suited for "counting" the isolated nuclei of molecules clustered within zeolite voids [5]. The MQ NMR pulse sequence forces the nuclear spins to act collectively via their dipolar couplings. ^{1}H MQ NMR studies found a maximum occupancy of two hexamethylbenzene molecules per supercage void in Na-Y at high loading [180].

NMR relaxation studies of molecular dynamics (section IV.B.4) necessarily include information on adsorbate distribution within the pore system. Stated differently, a correct interpretation of relaxation data requires a knowledge of distribution. Double quantum filtered ^{2}H NMR can be applied to adsorbates to detail molecular exchange processes and the distribution between different adsorption sites [125].

B. Reactive intermediates: charged or neutral

The transfer of a zeolite Bronsted proton to an adsorbed hydrocarbon is believed to be the first step in many catalytic reactions. The early steps of catalytic reactions are important since they involve complexation (chemisorption) with the active site and formation of the first intermediate. It is generally accepted that both oxygens around the aluminum

center are part of the active site, one acting as an acid and the other as a base [181].

The interactions of zeolite acid sites with simple molecules such as H_2O, CH_3OH and NH_3 have been studied in detail to determine if the adsorbate complexes are neutral (H-bonded) or ionic (proton transfer). Theoretical studies favor neutral complexes [24, 43], but a recent neutron diffraction study showed the existence of both protonated and H-bonded water in hydrated H-SAPO-34 at 25°C [182].

The adsorbate complexes formed by zeolite acid sites and olefins have also received considerable attention. They are difficult to study because of fast oligomerization reactions. Both IR and ^{13}C NMR are unable to resolve (or detect) olefinic moieties during the early moments of oligomerization [148]. This absence of olefins indicates that the interaction of with the acid center is either ionic (carbenium ions) or covalent (alkoxide) in nature.

Three-coordinate **carbenium ions** (carbocations) are often invoked as reactive intermediates in hydrocarbon transformations over acid catalysts. Alkyl ($^+C_nH_{2n+1}$) or alkenyl type ions ($^+C_nH_{2n-1}$) form over Bronsted or Lewis sites, respectively. Various types of carbenium ions have been generated in superacid solutions at low temperature and characterized by ^{13}C NMR in what has been termed "a triumph of organic chemistry" [183]. The transient nature of such ions on active catalytic surfaces would likely preclude NMR observation. In fact, only remarkably stable carbenium ions, such as alkyl-substituted cyclopentenyl [184], indanyl [185], triphenylmethyl [7, 186] and alkyl-substituted benzenium cations [170], have lifetimes sufficient for detection. Carbenium ions can persist in zeolites only if the zeolite is a stronger acid than the carbenium ion. As discussed above, zeolites such as H-ZSM-5 and H-Y are strong acids, but not superacids [100]. Benzenium cations were detected in H-ZSM-5 only because the co-product water was removed (using a flow reactor) after reacting methanol and benzene [170]. There is a general consensus that most carbenium ions do not exist (in significant equilibrium concentrations) *free* within the intracrystalline spaces of zeolites. Rather these ions interact strongly with the framework. Clearly, solvation phenomena are not possible for zeolites.

Framework-bound **alkoxy** species have been observed during olefin adsorption on acid zeolites by in-situ ^{13}C NMR [148, 152, 155]. Stepanov at al. concluded that the oligomers are bound as alkoxy species which are in rapid equilibrium with olefins and carbenium ions

[148]. They sustain that the concentrations of these latter species are beyond the sensitivity of NMR and IR spectroscopies.

Supposedly, these alkoxy species (Si-O-C_nH_{2n+1}) can be thought of as "incipient carbenium ions" forming during olefin protonation (or alcohol dehydration) which are captured by the nucleophilic framework oxygen [5, 152]. This idea is supported by the finding that zeolite lattice oxygens play an active role in catalysis [181]. Alkoxy complexes can exhibit carbenium-like properties. Stepanov and co-workers observed ^{13}C label scrambling, from the methyl groups of tert-butyl alcohol to the C-O group of *tert*-butoxy complexes, on H-ZSM-5 [155].

Theoretical quantum-chemical calculations show that carbenium ions are similar to excited transition states, not active intermediates. The energy required to rupture the covalent (O-C) bond in the alkoxy is compensated by the energy released during formation of the C-C bond in the product [182]. The important feature in such a concerted mechanism lies in the bifunctional nature of the active sites. One oxygen of the Brönsted acid moiety protonates (acidic) the olefin while the other (basic) bonds the electron-deficient carbon [24].

The role of alkoxides in the dehydration of butyl alcohols on H-ZSM-5 is controversial. Workers claim they are reactive intermediates [156] and stable side products [155].

C. Methanol to hydrocarbons

The methanol to gasoline conversion is one of the most successful routes to synthetic fuels. H-ZSM-5 operating at 370°C is the current leader for this process. The reactions of $^{13}CH_3OH$ on H-ZSM-5 were studied by in-situ ^{13}C MAS NMR using off-line heating [140, 141] and by temperature jump [146, 167]. Other adsorbates (alcohols and ethers) were also adsorbed in-situ to clarify longstanding questions in the mechanism. Key questions were: i) the mechanism of initial C-C bond formation, ii) which olefin is produced first, and iii) the reason for an induction period prior to hydrocarbon synthesis.

Extensive in-situ ^1H and ^{13}C NMR measurements have been made on this system. The adsorbed states of methanol on zeolites have been examined in detail by NMR spectroscopy [187, 188]. At low loadings (CH_3OH/acid site $\leq$ 1) methanol is adsorbed by hydrogen bonds, whereas at higher loadings methoxonium ions are present [188].

Haw's group made studies by increasing the temperature rapidly and acquiring data as a function of time (to compare kinetics [146]) or by raising the temperature in steps (to show reaction sequences [140]). At low temperature (25°C) the first catalytic steps were evidenced. A molecule of methanol is protonated, by the Brönsted acid sites of H-ZSM-5, before reacting with another methanol molecule to form dimethyl ether and water [141]. At 250°C the equilbrium between methanol, dimethyl ether, and water is maintained for ca. 30 minutes (induction period). At the onset of hydrocarbon formation (250°C) ethene and methyl ethyl ether were observed until the synthesis (isobutane and propane) was complete. Ethene is thus the first olefin formed.

The distribution of hydrocarbons in the adsorbed products at 300°C is very different from that in the desorbed products [141]. The expected thermodynamic equilibrium distribution of trimethylbenzenes were found in the adsorbed phase (in-situ ^{13}C NMR). However only the 1,2,4-trimethylbenzene isomer was desorbed (GC analysis). This isomer has the smallest kinetic diameter (0.61 nm). The other isomers, 1,2,3- and 1,3,5-trimethylbenzenes, have kinetic diameters too large (0.64 and 0.67 nm, respectively) to diffuse out of the channels of ZSM-5 at 300°C and must isomerize to 1,2,4-trimethylbenzene. Also, tetramethylbenzenes were found adsorbed but not desorbed. These findings are a direct observation of product shape selectivity.

D. Olefin oligomerization

The oligomerization of light olefins is an important process for making useful higher hydrocarbons such as gasolines (C_8), paraffins for synthesizing detergents (C_{11}-C_{14}), diesel fuels (C_{16}) and lubricants (C_{30}). More importantly, any processes involving olefins must cope with the negative effects of oligomerization which lead to catalyst deactivation.

Ethene ($^{13}C=^{13}C$) oligomerization has been examined by several groups [146–148]. Haw and co-workers used variable temperature (up to 400°C) in-situ ^{13}C MAS NMR spectroscopy to study ethene oligomerization and cracking [146]. The first active intermediate formed was not detected. At 25°C linear oligomers are rapidly formed. Heating to 250°C caused the oligomers to be cracked to propanes, butanes and higher aliphatics. A small amount of aromatics and cyclopentenyl carbenium ions were also observed. At 350°C the products were meth-

ane, ethane, propane and methyl-substituted benzenes. The cyclopentenyl cations were converted to aromatics.

Datema's group studied the acid-catalyzed oligomerization of ^{13}C enriched ethene over several catalysts, but at lower temperatures [147]. Alkoxy species were detected and theorized to be intermediates in the reaction. After short times at 0°C reactive olefins were observed that subsequently reacted to form paraffins. The branchiness of the final products is correlated with the dimensions of the pore systems. More linear products are obtained from the medium pore zeolite H-ZSM-5. Large pore catalysts H-MOR and H-Y gave much more branched oligomers.

E. Catalyst deactivation

Industrial catalysts used world-wide are not *true* catalysts by definition, in the sense that they are modified irreversibly during use. Catalyst deactivation is a costly phenomenon caused by the formation and retention of heavy secondary products within the pore system. It is one of the major economic problems in the chemical industry. Zeolites are regenerated, when the activity drops below a certain level, by burning or washing the deposits off.

In deactivation, the organic deposits prohibit contact between the reagent molecule and the active site (bridging hydroxyl group). This can occur by physical blockage (steric repulsion) or by chemical poisoning (strong chemisorption). In-situ characterization of the deposites is important since they are usually too large to desorb without fragmentation. Any attempt to remove them from the cavities (for ex-situ analysis) will usually cause some chemical transformation.

NMR spectroscopy has been applied to characterize the organic deposits and to understand how and where they form [189–191]. The structures of the deposits are determined mainly by the size and shape of zeolite cavities and apertures, rather than the acidity. In zeolites with a mono-dimensional pore system (e.g. MOR) deactivation is rapid since one organic molecule (deposit) can block numerous active sites. Three-dimensional pore systems (e.g. ZSM-5, Y) exhibit slower deactivation since the one organic molecule poisons one active site. The ease of regeneration is inversely related to the rate of coking. ZSM-5 is very resistant to deactivation and it is very difficult to regenerate.

As mentioned above, NMR studies found the oligomerization of olefins at room temperature and low dosing (on strong acid catalysts) to yield molecules with only paraffinic carbons. This indicates the formation of cyclic alkanes or species which remain strongly adsorbed (thus, no generation of unsaturated moities). Otherwise, one cannot explain the coupling of olefinic molecules to produce purely saturated species.

Most reported NMR studies of deactivation involve the formation of carbonaceous deposits above 200°C [189]. At these temperatures cracking reactions occur to form alkylaromatics. Above 500°C the deposits are totally aromatic or graphitic. ^{13}C MAS NMR studies show that the amount of NMR invisible carbon increases as the amount of coke (high temperature deposits) increases. Loss of NMR signal is due to signal broadening caused by organic free radicals (aromatic) or conducting electrons (graphite). Thus, only catalysts with low amounts of organic deposits can be characterized by NMR. UV-visible spectroscopy is a better choice for studying these systems.

VI. CONCLUDING REMARKS AND FUTURE PROSPECTS

NMR studies of zeolite catalysis are numerous and they will certainly continue to grow in a pronounced manner. The studies can be conceptually divided into three parts involving characterization of zeolite: 1) structure, 2) acidity and 3) catalyzed organic reactions.

XRD is the principal method for determining zeolite structure. However, NMR spectroscopy has great advantages over XRD for studying the active site structures in zeolites: 1) studies of selected nuclei are possible by NMR methods, and 2) the chemical nature of the various nuclei are evidenced. In addition, NMR spectroscopy is readily applied to amorphous catalysts (which were not mentioned here).

The National Research Council recently concluded that in-situ spectroscopic studies of catalytic reactions have the highest priority for understanding catalysis [192]. NMR is especially advantageous among the spectroscopic techniques for the following reasons.

- It is well suited for determining both the molecular structures *and* dynamics of small adsorbed organic molecules. Applied along with selected probe molecules, NMR studies can give detailed information on zeolite acidity and reaction mechanisms.

- A wide variety of selective and correlated double resonance experiments are possible. These experiments can be applied directly to the dry zeolite or, more interestingly, to zeolites loaded with specific probe molecules, or the reagents of interest, to give detailed structural information on the adsorbate-adsorbent complexes (e.g. ^{13}C-^{27}Al distances).
- NMR spectroscopy can be applied under in-situ conditions.

Two recent important technological breakthroughs will greatly enhance these advantages: 1) The detection of quadrupolar ^{27}Al nuclei by the MQ MAS NMR method provides a much needed resolution of spectra for this nucleus with high catalytic importance. 2) Realistic in-situ conditions with reagent flow for samples undergoing MAS. This breakthrough will stimulate the growth of mechanistic studies.

Zeolites are commercially indispensable as solid acids since their *acidity*(strength, concentration) and *pore structure* can be tailored for specific reactions of adsorbed organic molecule. NMR studies of zeolites have provided new insights into solid Bronsted acidity (e.g. characterization) and have revealed, for the first time, the importance of the pore structure in the catalytic proton transfer reaction. NMR work will surely continue to enhance our knowledge of solid acidity in the future from various perspectives (e.g. effective strength of an acid site in the presence of a specific adsorbate, motional state of the molecule interacting with the active site). Investigations of Lewis acidity and basicity by NMR methods are also expected to yield important discoveries in the near future.

NMR studies, in combination with computer modelling, will be important for rationalizing and tailoring the shape-selectivity properties of zeolites. The shape-selectivity of a reaction is determined by the dimensions of the intracrystalline pores *and* the reacting molecules present. Analysis of the reacting species requires, again, in-situ spectroscopic methods.

References

1. W.M. Meier, D.H. Olson and Ch. Baerlocher, Zeolites, *17*, Al (1996).
2. R. Szostak in "Molecular Sieves: Principles of Synthesis and Identification", VNR, New York (1989).
3. "Catalysis and Zeolites", J. Weitkamp, L. Puppe, Eds., Springer-Verlag, Berlin (1999).
4. A. Corma, Chem. Rev., *95*, 559 (1995).

5. "NMR Techniques in Catalysis", A.T. Bell, A. Pines, Eds., Marcel Dekker, New York (1994).
6. C.M. Csicsery, Zeolites, *4*, 202 (1984).
7. M.L. Cano, A. Corma, V. Fornes, H. Garcia, M.A. Miranda, C. Baerlocher, C. Lengauer, J. Am. Chem. Soc., *118*, 11006 (1996).
8. High-Resolution Solid-State NMR on Silicalites and Zeolites", G. Engelhardt, D. Michel, Eds., Wiley, New York (1987).
9. J. Klinowski, Chem. Rev., *91*, 1459 (1991).
10. H. Pfeifer, NMR Basic Principles and Progress, *31*, 31 (1994); H. Pfeifer, H. Ernst, Annual Reports on NMR Spectroscopy, *28*, 91 (1994).
11. M. Stocker, Stud. Surf. Sci. Catal., *85*, 429 (1994).
12. M.M. Maricq and J.S. Waugh, J. Chem. Phys. *70*, 3300 (1979).
13. "Modern NMR Techniques and Their Application in Chemistry", A.I. Popov, K. Hallenga, Eds., Marcel Dekker, New York (1991).
14. X. Teng, J.F. Haw, Top. Catal., *4*, 109 (1997).
15. M. Hunger and T. Horvath, J. Chem. Soc., Chem. Commun. 1423 (1995).
16. M. Hunger and T. Horvath, J. Catal., *167*, 187 (1997).
17. P. Goguen, J.F. Haw, J. Catal., *161*, 870 (1996).
18. E. MacNamara, D. Raftery, J. Catal., *175*, 135 (1998).
19. M. Hunger, M. Seiler, T. Horvath, Catal. Lett., *57*, 199 (1999).
20. M. Hunger, T. Horvath, J. Weitkamp, Microporous & Mesoporous Materials, *22*, 357 (1998).
21. P.K. Isbester, A. Zalusky, D.H. Lewis, M.C. Douskey, M.J. Pomije, K.R. Mann, E.J. Munson, Catal. Today, *49*, 363 (1999).
22. I.I. Ivanova and E.G. Derouane, Stud. Surf. Sci. Catal., *85*, 357 (1994).
23. W.E. Farneth, R.J. Gorte, Chem. Rev., *95*, 615 (1995).
24. R.A. van Santen, Chem. Rev., *95*, 637 (1995).
25. "Acid-Base Catalysis II", Stud. Surf. Sci. Catal., *90* (1994).
26. J.F. Haw, J.B. Nicholas, T. Xu, L.W. Beck and D.B. Ferguson, Acc. Chem. Res., *29*, 259 (1996); J.F. Haw, J.B. Nicholas, Stud. Surf. Sci. Catal., *101*, 573 (1996).
27. G.J. Gajda and J.A. Rabo, in "Acidity and Basicity of Solids", eds. J. Fraissard, L. Petrakis, Kluwer Academic, Amsterdam (1994) p. 127.
28. R.A. van Santen, Stud. Surf. Sci. Catal., *85*, 273 (1994).
29. H. Ernst, D. Freude and I. Wolf, Chem. Phys. Lett. *212*, 588 (1993); D. Freude, H. Ernst and I. Wolf, Solid State NMR. *3*, 271 (1994).
30. M. Hunger, Solid State NMR, *6*, 1 (1996).
31. M. Hunger, Catal. Rev. Sci. Eng., *39*, 345 (1997).
32. C. Lee, D.J. Parrillo, R.J. Gorte, W.E. Farneth, J. Am. Chem. Soc., *118*, 3262 (1996).
33. J. Sauer, C.M. Kolmel, J.-R. Hill, R. Ahlrichs, Chem. Phys. Lett., *164*, 193 (1989); J. Sauer in "Modelling of Structure and Reactivity in Zeolites", ed. C.R.A. Catlow, Academic, New York (1992).
34. W.J. Mortier, J. Sauer, J.A. Lercher, H. Noller, J. Phys. Chem., *88*, 905 (1984).
35. D. Freude, J. Klinowski, J. Chem. Soc. Chem. Commun., 1411 (1988); D. Freude, J. Klinowski, H. Hamdan, Chem. Phys. Lett., *149*, 355 (1988).
36. J.M. Kobe, T.J. Gluszak, J.A. Dumesic and T.W. Root, J. Phys. Chem. *99*, 5485 (1995).
37. M. Czjzek, H. Jobic, A.N. Fitch, T. Vogt, J. Phys. Chem., *96*, 1535 (1992).
38. M. Hunger, M.W. Anderson, A. Ojo, H. Pfeifer, Microporous Materials, *1*, 17 (1993).
39. P. Sarv, T. Tuherm, E. Lippmaa, K. Keskinen, A. Root, J. Phys. Chem., *9*, 13763 (1995).

40. J. Dwyer in "Zeolite Microporous Solids: Synthesis, Structure and Reactivity", eds. E.G. Derouane et al., Kluwer Academic (1992), p. 303.
41. F. Deng, Y. Yue, C. Ye, Solid State NMR, *10*, 151 (1998).
42. G.L. Woolery, G.H. Kuehl, H.C. Timken, A.W. Chester, J.C. Vartuli, Zeolites, 19, 288 (1997).
43. U. Eichler, M. Brandle, J. Sauer, J. Phys. Chem. B, *101*, 10035 (1997); J. Sauer, Science, 271, 774 (1996); F. Haase, J. Sauer, J. Phys. Chem., *98*, 3083 (1994).
44. D. Farcasiu, A. Ghenciu, J. Prog. Nucl. Magn. Reson., *29*, 129 (1996).
45. D. Farcasiu, D. Hancu, Catal. Lett., *53*, 3 (1998); D. Farcasiu, J. Catal., *167*, 303 (1997).
46. A. Pines, G. Gibby, J.S. Waugh, J. Chem. Phys., *56*, 1776 (1972); *59*, 569 (1973).
47. P. Bodart, J.B. Nagy, G. Debras, Z. Gabelica, P.A. Jacobs, J. Phys. Chem., *90*, 5183 (1986).
48. G.T. Koktailo, C.A. Fyfe, Y. Feng, H. Grondey, H. Gies, B. Marler, D.E. Cox, Stud. Surf. Sci. Catal., *94*, 78 (1995).
49. C.A. Fyfe, Y. Feng, H. Grondey, G.T. Kokotailo, *91*, 1525 (1991).
50. C.A. Fyfe, J.H. O'Brien, H. Strobl, Nature, *326*, 281 (1987).
51. C.A. Fyfe, Y. Feng, H. Gies, H. Grondey, G.T. Kokotailo, J. Am. Chem. Soc., *112*, 3264 (1990); C.A. Fyfe, H. Grondey, Y. Feng, G.T. Kokotailo, J. Am. Chem. Soc., *112*, 8812 (1990).
52. M.T. Weller, S.E. Dann, G.M. Johnson, P.J. Mead, Stud. Surf. Sci. Catal., *105*, 455 (1997).
53. R.J. Kirkpatrick and B.L. Phillips, Appl. Magn. Reson. *4*, 213 (1993).
54. R. Gougeon, L. Delmotte, D. Le Nouen, Z. Gabelica, Microporous & Mesporous Materials, *26*, 143 (1998).
55. S.D. Kinrade, C.T.G. Knight, D.L. Pole, R.T. Syvitski, Inorg. Chem., *37*, 4272 (1998); ibid, *37*, 4278.
56. C.E.A. Kirschhock, R. Ravishankar, F. Verspeurt, P.J. Grobet, P.A. Jacobs, J.A. Martens, J. Phys. Chem., *103*, 4965 (1999); C.E.A. Kirschhock, R. Ravishankar, L. Van Looveren, P.A. Jacobs, J.A. Martens, J. Phys. Chem., *103*, 4972 (1999).
57. D.R. Kinney, I.S. Chuang and G.E. Maciel, J. Am. Chem. Soc. *115*, 6786 (1993).
58. M. Hunger, S. Ernst and J. Weitkamp, Zeolites, *15*, 188 (1995).
59. H. Koller, R.F. Lobo, S.L. Burkett, M.E. Davis, J. Phys. Chem., *99*, 12588 (1995).
60. E. Brunner, H.G. Karge and H. Pfeifer, Z. Phys. Chem. (Munich) *176*, 173 (1992).
61. E. Brunner, U. Sternberg, J. Prog. NMR Spectros., *32*, 21 (1998).
62. T. Baba, N. Komatsu, Y. Ono, H. Sugisawa, T. Takahasi, Microporous Mesoporous Materials, *22*, 203 (1998).
63. G. Engelhardt, W. Veeman, J. Chem. Soc. Chem. Commun, 622 (1993).
64. H. Koller, E.L. Meijer, R.A. van Santen, Solid State NMR, *9*, 165 (1997).
65. C.P. Grey and A.J. Vega, J. Am. Chem. Soc. *117*, 8232 (1995).
66. L.C. de Menorval, W. Buckermann, F. Figueras, F. Fajula, J. Phys. Chem., *100*, 465 (1996).
67. A. Samoson, Chem. Phys. Lett., *119*, 29 (1985).
68. C. Jager, NMR Basic Principles and Progress, *31*, 133 (1994); G. Kunath-Fandrei, T.J. Bastow, J.S. Hall, C. Jager, M.E. Smith, J. Phys. Chem. *99*, 15138 (1995).
69. E. Lippmaa, A. Samoson, M. Magi, J. Am. Chem. Soc., *108*, 1730 (1986).
70. W. Kolodziejski, A. Corma, Solid State NMR, *3*, 177 (1994).
71. L. Kellberg, M. Linsten, H.J. Jakobsen, Chem. Phys. Lett., *182*, 120 (1991).
72. J. Haase, E. Oldfield, Solid State NMR, *3*, 171 (1994).
73. L.W. Beck and J.F. Haw, J. Phys. Chem. *99*, 1076 (1995).
74. A.L. Blumenfeld, D.J. Coster and J.J. Fripiat, Chem. Phys. Lett., *231*, 491 (1994).

75. J.M. Griffiths, R.G. Griffin, Anal. Chim. Acta., *283*, 1081 (1993); T. Guillon, J. Schaefer, in W.S. Warren (Eds.), Advances in Magnetic Reson., vol. 13, Academic Press, New York (1989), p. 57.
76. C.A. Fyfe, K.C. Wong-Moon, Y. Huang, H. Grondey, K.T. Mueller, J. Phys. Chem., *99*, 8707 (1995).
77. L. van Wullen, Solid State NMR, *13*, 123 (1998).
78. L. Frydman and J.S. Harwood, J. Am. Chem. Soc. *117*, 5367 (1995); A. Medek, J.S. Harwood, L. Frydman, J. Am. Chem. Soc. *117*, 12779 (1995).
79. T. Vosegarrd, F.H. Larsen, H.J. Jakobsen, P.D. Ellis, N.C. Nielsen, J. Am. Chem. Soc., *119*, 9055 (1997).
80. J.-P. Amoureux, C. Fernandez, S. Steuernagel, J. Magn. Reson., *123*, 116 (1996).
81. J.-P. Amoureux, C. Fernandez, Solid State NMR, *10*, 211 (1998).
82. G. Wu, D. Rovnyak, R.G. Griffin, J. Am. Chem. Soc., *118*, 9326 (1996).
83. C. Fernandez, L. Delevoye, J.-P. Amoureux, D.P. Lang, M. Pruski, J. Am. Chem. Soc., *119*, 6858, 1997.
84. M. Pruski, C. Fernandez, D.P. Lang, J.-P. Amoureux; Catal. Today, *49*, 401 (1999).
85. P. Sarv, C. Fernandez, J.-P. Amoureux, K. Keskinen, J. Phys. Chem., *100*, 19223 (1996).
86. A. Samoson, E. Lippmaa and A. Pines, Mol. Phys., *65*, 1013 (1988).
87. K.T. Mueller, B.Q. Sun, G.C. Chingas, J.W. Zwanziger, T. Terao and A. Pines, J. Magn. Reson., *86*, 470 (1990).
88. E.G. Derouane, H. He, S.B. Derouane-Abd Hamid, I.I. Ivanova, Catal. Lett., *58*, 1 (1999).
89. I.J.F. Poplett, M.E. Smith, Solid State Nucl. Magn. Reson., *11*, 211 (1998).
90. X. Wu, L.G. Butler, Microporous Materials, *4*, 265 (1995).
91. M. Hunger, S. Ernst, S. Steuernagel and J. Weitkamp, Microporous Materials, *6*, 349 (1996).
92. H.K.C. Timken, G.L. Turner, J.P. Gilson, L.B. Welsh, E. Oldfield, J. Am. Chem. Soc., *108*, 7231 (1986).
93. P.J. Dirken, S.C. Kohn, M.E. Smith, E.R.H. van Eck, Chem. Phys. Lett., *266*, 568 (1997).
94. Z. Xu, J.F. Stebbins, Solid State NMR, *11*, 243 (1998).
95. U.-T. Pingel, J.-P. Amoureux, T. Anupold, F. Bauer, H. Ernst, C. Fernandez, D. Freude, A. Samoson, Chem. Phys. Lett., *294*, 345 (1988).
96. P. Batamack, C. Doremieux-Morin, R. Vincent and J. Fraissard, J. Phys. Chem., *97*, 9779, (1993).
97. L. Heeribout, V. Semmer, P. Batamack, C. Dorémieux-Morin, R. Vincent and J. Fraissard, Stud. Surf. Sci. Catal., *101*, 831 (1996).
98. D. Farcasiu, D. Hancu, J. Chem. Soc. Faraday Trans., *93*, 2161 (1997).
99. D. Farcasiu and A. Ghenciu, J. Am. Chem. Soc. *115*, 10901 (1993).
100. T. Xu, E.J. Munson and J.F. Haw, J. Am. Chem. Soc. *116*, 1962 (1994).
101. J.F. Haw, M.B. Hall, A.E. Alvarado-Swaisgood, E.J. Munson, Z. Lin, L.W. Beck, T. Howard, J. Am. Chem. Soc. *116*, 7308 (1994).
102. G.A. Olah, T.E. Kiovsky, J. Am. Chem. Soc., *90*, 4666 (1968).
103. J. Sepa, R.J. Gorte, D. White, B.H. Suits, V.S. Swaminathan, Proc. of 12th International Zeolite Conference, Materials Research Society, Warrendale, PA (1999) p. 2287.
104. V. Bosacek, H. Ernst, D. Freude, T. Mildner, Zeolites, *18*, 196 (1997); V. Bosacek, J. Phys. Chem. *97*, 10732 (1993).
105. H. Sachsenroder, E. Brunner, M. Koch, H. Pfeifer and B. Staudte, Microporous Materials, *6*, 341 (1996).
106. E. Brunner, H. Pfeifer, Anal. Methods Instrumentation, *2*, 315 (1995).

107. J.A. Ripmeester, J. Am. Chem. Soc., *105*, 2925 (1983).
108. D. Coster, L. Blumenfeld, J.J. Fripiat, J. Phys. Chem., *98*, 6201 (1994).
109. V.M. Mastikhin, J.L. Mudrakowsky, S.V. Filimonova, Chem. Phys. Lett., *149*, 175 (1988).
110. A. Simon, L. Delmotte, J.-M. Chezeau, L. Huve, J. Chem. Soc. Chem. Commun., 263 (1997).
111. J.H. Lunsford, Top. Catal., *4*, 91 (1997); J.H. Lunsford, P.N. Tutunjian, P.-j. Chu, E.B. Yeh, D.J. Zalewski, J. Phys. Chem., *93*, 2590 (1989).
112. B. Zhao, H. Pan, J.H. Lunsford, Langmuir, *15*, 2761 (1999).
113. E.F. Rakiewicz, A.W. Peters, R.F. Wormsbecher, K.J. Sutovich, K.T. Mueller, J. Phys. Chem. *102*, 2890 (1998).
114. K.J. Sutovich, A.W. Peters, E.F. Rakiewicz, R.F. Wormsbecher, S.M. Mattingly, K.T. Mueller, J. Catal., *183*, 155 (1999).
115. J.P. Osegovic, R.S. Drago, J. Catal. *182*, 1 (1999).
116. H.-M. Kao, C.P. Grey, J. Magn. Reson., *133*, 313 (1998); H.-M. Kao, C.P. Grey, J. Am. Chem. Soc., *119*, 627 (1997).
117. L.W. Beck, T. Xu, J.B. Nicholas, J.F. Haw, J. Am. Chem. Soc., *117*, 11594 (1995).
118. T. Mildner, D. Freude, J. Catal., *178*, 309 (1998).
119. G. Bourdillion, C. Gueguen and M. Guisnet, Appl. Catal. *61*, 123 (1990).
120. W.O. Parker, Jr., Stud. Surf. Sci. Catal., 94, 568 (1995).
121. C. Flego, W.O. Parker, Jr., Applied Catal. A, *185*, 137 (1999).
122. T.M. Duncan in "Elementary Reaction Steps in Heterogeneous Catalysis" (R.W. Joyner and R.A. van Santen, Eds.), Kluwer Academic, Amsterdam, 1993, p. 221.
123. D.J. Schaefer, D.E. Favre, M. Wilhelm, S.J. Weigel, B.F. Chmelka, J. Am. Chem. Soc., *119*, 9252 (1997).
124. S.M. Auerbach, L.M. Bull, N.J. Henson, H.I. Metiu, A.K. Cheetham, J. Phys. Chem., *100*, 5923 (1996).
125. Y.-H. Chen, W.-T. Chang, P.-C. Jiang, L.-P. Hwang, Microporous & Mesoporous Materials, *21*, 651 (1998).
126. U. Schwerk, D. Michel, J. Phys. Chem., *100*, 352 (1996).
127. F.G. Riddell, S. Arumugam, K.D.M. Harris, M. Rogerson, J.H. Strange, J. Am. Chem. Soc., *115*, 1181 (1993).
128. H.W. Spiess in "Advances in Polymer Science", eds. H.H. Kausch, H.G. Zachmann, Springer-Verlag, Berlin (1985), vol. 66, p. 23.
129. "Multidimensional Solid-State NMR and Polymers", eds. K. Schmidt-Rohr, H.W. Spiess, Academic Press, London (1994).
130. L.M. Bull, S.J. Heyes, A.K. Cheetham, Proceedings of 9th Intl. Zeolite Conference, Eds. R. von Ballmooos et al., Butterworth Heinemann, (1993), p. 63; R.L. Portsmouth, M.J. Duer, L.F. Gladden, ibid, p. 37.
131. I. Kustanovich, Z. Luz, S. Vega, A.J. Vega, J. Phys. Chem., *94*, 3138 (1990).
132. A.E. Aliev, K.D.M. Harris, F. Guillaume, J. Phys. Chem., *99*, 1156 (1995).
133. D. Farcasiu, P. Lukinskas, A. Ghenciu, R. Martin, J. Molc. Catal. A, *137*, 213 (1999).
134. J. Jeener, B.H. Meier, P. Bachmann, R.R. Ernst, J. Chem. Phys., *71*, 4546 (1979).
135. "Principles of NMR in One and Two Dimensions", R.R. Ernst, G. Bodenhausen, A. Wokaun, Clarendon Press, Oxford (1987).
136. A. Heuer, J. Leisen, S.C. Kuebler, H.W. Spiess, J. Chem. Phys., *105*, 7089 (1996).
137. H.B. Schwarz, S. Ernst, J. Karger, B. Knorr, G. Seiffert, R.Q. Snurr, B. Staudte, J. Weitkamp, J. Catal., *167*, 248 (1997); H. Jobic, H. Ernst, W. Heink, J. Karger, A. Tuel, M. Bee, Microporous & Mesoporous Materials, *26*, 67 (1998).
138. R.Q. Snurr, A. Hagen, H. Ernst, H.B. Schwarz, S. Ernst, J. Weitkamp, J. Karger, J. Catal., *163*, 130 (1996).

139. N.D. Lazo, D.K. Murray, M.L. Kieke and J.F. Haw, J. Am Chem. Soc. *114*, 8552 (1992).
140. E.J. Munson, A.A. Kheir, N.D. Lazo and J.F. Haw, J. Phys Chem. *96*, 7740 (1992).
141. M.W. Anderson and J. Klinowski, Nature *339*, 200 (1989).
142. M.D. Alba, A.A. Romero, M.L. Occelli and J. Klinowski, J. Phys. Chem. B, *101*, 5166 (1997).
143. P.W. Goguen, T. Xu, D.H. Barich, T.W. Skloss, W. Song, Z. Wang, J.B. Nicolas, J.F. Haw, J. Am. Chem. Soc., *120*, 2650 (1998).
144. M.W. Anderson, B. Sulikowski and P.J. Barrie, J. Phys. Chem., *94*, 2730 (1990).
145. Y. Xu, C.P. Grey, J.M. Thomas and A.K. Cheetham, Catal. Lett. *4*, 251 (1990).
146. F.G. Oliver, E.J. Munson and J.F. Haw, J. Phys. Chem. *96*, 8106 (1992).
147. K.P. Datema, A.K. Nowak, J. van Braam Houckgeest and A.F.H. Wielers, Catal. Lett., *11*, 267 (1991).
148. A.G. Stepanov, M.V. Luzgin, V.N. Romannikov, V.N. Sidelnikov, E.A. Paukshtis, J. Catal., *178*, 466 (1998).
149. Y.S. Kye, S.X. Wu and T.M. Apple, J. Phys. Chem. *96*, 2632 (1992).
150. I.I. Ivanova, A.I. Rebrov, E.B. Pomakhina, E.G. Derouane, J. Molc. Catal. A, *141*, 107 (1999).
151. E.G. Derouane, S.B. Abdul Hamid, I.I. Ivanova, N. Blom and P.E. Hojlund-Nielsen, J. Mol. Catal., *86*, 371 (1994).
152. J.F. Haw, B.R. Richardson, I.S. Oshiro, N.D. Lazo and J.S. Speed, J. Am. Chem. Soc., *111*, 2052, (1989).
153. C.H.S. Chen and R.F. Bridger, J. Catal., *161*, 687 (1996).
154. M.W. Anderson, J. Dwyer, G.J. Hutchings, D.F. Lee, M. Makarova, B. Zibrowius, Catal. Lett. *31*, 377 (1995).
155. A.G. Stepanov, Catal. Today *24*, 341 (1995); A.G. Stepanov, K.I. Zamaraev and J.M. Thomas, Catal. Lett. *13*, 407 (1992).
156. M.T. Aronson, R.J. Gorte and W.E. Farneth, J. Am. Chem. Soc., *111*, 840 (1989).
157. N.D. Lazo, et al., J. Phys. Chem. *95*, 9420 (1991).
158. B.R. Richardson, N.D. Lazo, P.D. Schettler, J.L. White and J.F. Haw, J. Am. Chem. Soc. *112*, 2886 (1990).
159. I.I. Ivanova, A. Pasau-Claerbout, M. Seirvert, N. Bloom and E.G. Deroune, J. Catal. *158*, 521 (1996).
160. A. Philippou, M.W. Anderson, J. Catal., *158*, 385 (1996).
161. I.I. Ivanova, D. Brunel, J.B. Nagy and E.G. Derouane, J. Mol. Catal. *95*, 243 (1995).
162. I.I. Ivanova and A. Corma, J. Phys. Chem. B, *101*, 547 (1997).
163. A. Philippou, M.W. Anderson, J. Am. Chem. Soc., *116*, 5774 (1994).
164. M. Hunger, U. Schenk, J. Weitkamp, J. Molc. Catal. A, *134*, 97 (1998).
165. A. Philippou, M.W. Anderson, J. Catal., *167*, 266 (1997).
166. T. Mildner, H. Ernst, D. Freude, W.F. Holderich, J. Am. Chem. Soc., *119*, 4258 (1997).
167. H. Ernst, D. Freude, T. Mildner, I. Wolf, Solid State NMR, *6*, 147 (1996).
168. T. Miyoshi, K. Takegoshi and T. Terao, J. Magn. Reson., *125*, 383 (1997).
169. C. Keeler, J. Xiong, H. Lock, S. Dec, T. Tao, G.E. Maciel, Catal. Today, *49*, 377 (1999).
170. T. Xu, D.H. Barich, P.W. Goguen, W. Song, Z. Wang, J.B. Nicholas, J.F. Haw, J. Am. Chem. Soc., *120*, 4025 (1998).
171. J.F. Haw, P.W. Goguen, T. Xu, T.W. Skloss, W. Song, Z. Wang, Angew. Chem. Int. Ed., *37*, 948 (1998).
172. P.K. Wang, C.P. Slichter, J.H. Sinfelt, J. Phys. Chem., *89*, 3606 (1985).
173. T. Gullion, Concepts. Magn. Reson., *10*, 277 (1998); T. Gullion, J. Schaefer, Adv. Magn. Reson., *13*, 57 (1989).

174. Z. Gan, J. Am. Chem. Soc., *114*, 8307 (1992).
175. J.Z. Hu, W. Wang, F. Liu, M.S. Solum, D.W. Alderman, R.J. Pugmire, D.M. Grant, J. Magn. Reson., *113*, 210 (1995).
176. A. Philippou, F. Salehirad, D.P. Luigi, M.W. Anderson, 12th International Zeolite Conference, p. 2465 (1999).
177. J. Gottwald, D.E. Demco, R. Graf, H.W. Spiess, Chem. Phys. Lett., *243*, 314 (1995).
178. K. Inumaru, N. Jin, S. Uchida, M. Misono, J. Chem. Soc. Chem. Commun., 1489 (1998).
179. W. Kolodziejski, J. Klinowski, Appl. Catal. A, *81*, 133 (1992).
180. B.F. Chmelka, J.G. Pearson, S.-B. Liu, R. Ryoo, L.C. de Menorval, A. Pines, J. Phys. Chem., *95*, 303 (1991).
181. G.J. Kramer, R.A. van Santen, C.A. Emeis and A.K. Nowak, Nature, *363*, 529 (1993).
182. L. Smith, A.K. Cheetham, R.E. Morris, L. Marchese, J.M. Thomas, P.A. Wright, J. Chen, Science, *271*, 799 (1996).
183. V.B. Kazansky and I.N. Senchenya, J. Molc. Catal. *74*, 257 (1992).
184. "Superacids", G.A. Olah, G.K. Surya Prakash and J. Sommer, Wiley & Sons, New York, 1985. G.A. Olah and D.J. Donovan, J. Am. Chem. Soc. *99*, 5026 (1977).
185. T. Xu and J.F. Haw, J. Am. Chem. Soc. *116*, 7753 (1994).
186. T. Xu and J.F. Haw, J. Am. Chem. Soc. *116*, 10188 (1994).
187. T. Tao and G.E. Maciel, J. Am. Chem. Soc., *117*, 12889 (1995).
188. M. Hunger, T. Horvath, J. Am. Chem. Soc., *118*, 12302 (1996).
189. F. Salehirad, M.W. Anderson, J. Catal., *177*, 189 (1998); A. Thursfield, M.W. Anderson, J. Phys. Chem., *100*, 6698 (1996).
190. J.L. Bonardet, M.C. Barrage and J. Fraissard, J. Mol. Catal. A, *96*, 123 (1995).
191. M. Guisnet, P. Magnoux, D. Martin, in "Catalyst Deactivation", eds. C.H. Bartholomew, G.A. Fuentes, Elsevier Science, Amsterdam (1997), p. 1.
192. T. Ito, J.L. Bonardet, J. Fraissard, J.B. Nagy, C. Andre, Z. Gabelica, E.G. Derouane, Appl. Catal., *43*, L5 (1988).
193. National Resarch Council, "Catalysis Looks to the Future", National Academy Press, Washington D.C. (1992).